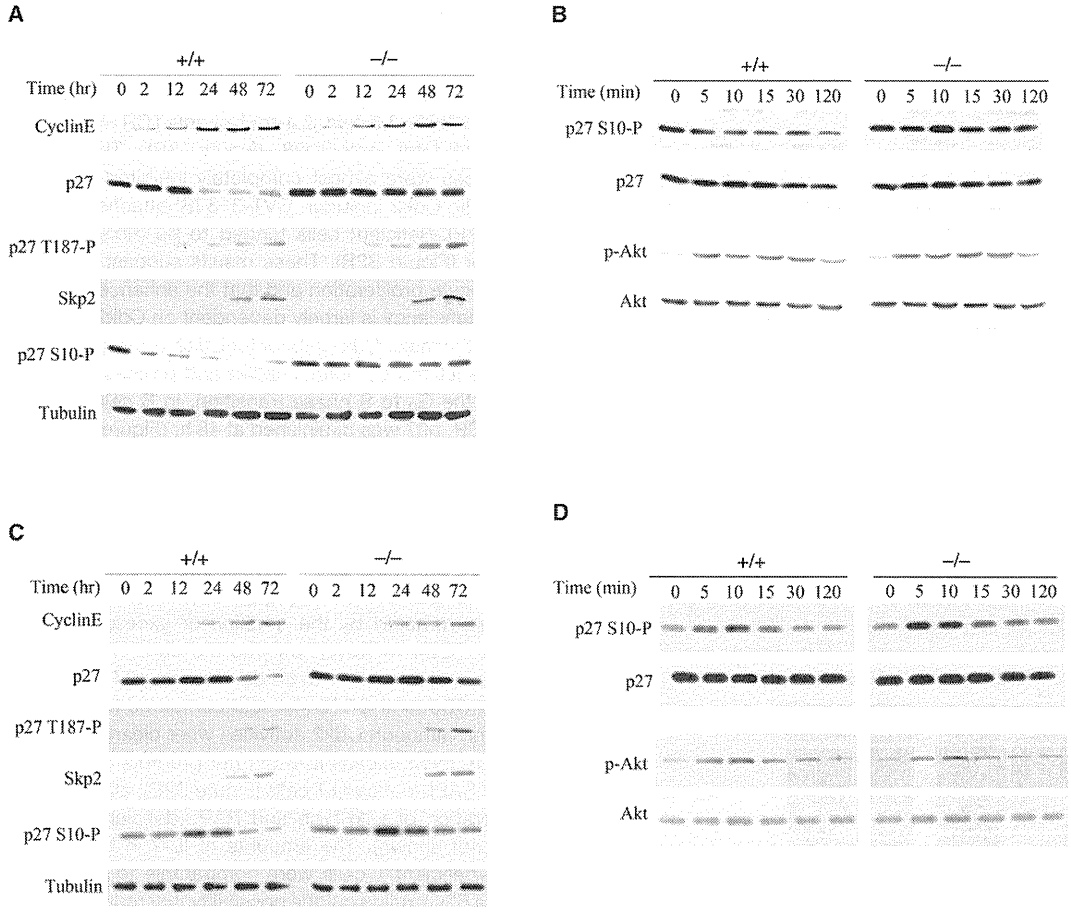

Figure 4. Deregulation of p27 in RAPL-Deficient Lymphocytes

(A) Defective p27 downregulation in RAPL-deficient B cells. Wild-type (+/+) and RAPL-deficient (−/−) B cells were stimulated with anti-IgM F(ab')$_2$ for the indicated times, followed by immunoblot analysis of cyclin E, p27, phosphorylated p27 at threonine 187, Skp2, phosphorylated p27 at serine 10, and tubulin. Total lysates from 1 × 10^5 cells were applied in each lane.

(B) Kinetics of p27 phosphorylation at serine 10 (S10) in wild-type (+/+) and RAPL-deficient (−/−) B cells after anti-IgM stimulation. Total and S10 phosphorylated p27 and total and phosphorylated Akt are shown. Total lysates from 1 × 10^5 cells were applied.

(C) Defective p27 downregulation in RAPL-deficient T cells. Wild-type (+/+) and RAPL-deficient (−/−) T cells were stimulated with anti-CD3 and anti-CD28 for the indicated times, followed by immunoblot analysis as in (A).

(D) Kinetics of p27 phosphorylation at serine 10 (S10) in wild-type (+/+) and RAPL-deficient T cells (−/−) after anti-CD3 and anti-CD28 stimulation. Total and S10 phosphorylated p27 and total and phosphorylated Akt are shown. Total lysates from 1 × 10^5 cells were applied.

renders it inaccessible to a complex of cyclin E and Cdk2, leading to enhanced Cdk2 activities and resistance to degradation.

In all B cell lymphoma generated in RAPL-deficient mice, p27 was abundantly present in the cytoplasm (Figure 3D), as observed in BCR-stimulated RAPL-deficient B blasts (Figure 3C). Line-profile analysis showed that 87.6% ± 3.7% of p27 was present in the cytoplasm. This suggests that the mislocalization of p27 in the cytoplasm underlies lymphoma development.

Kinetics of Phosphorylation and Degradation of p27 in RAPL-Deficient Cells

To investigate whether the mislocalization of p27 in the cytoplasm underlies lymphoproliferative disorders, we examined p27 degradation in more detail. In wild-type B and T cells, p27 declined sharply between 24 and 48 hr after antigen receptor stimulation (Figures 4A and 4C). Cyclin E increased after 12–24 hr and was maintained at high amounts at 24–72 hr. In contrast, RAPL-deficient cells maintained high p27 even at 72 hr poststimulation, whereas cyclin E upregulation was comparable to that in wild-type cells. T187 phosphorylation of p27, a trigger of p27 downregulation, was detected in wild-type cells at 24–72 hr, which coincided with the kinetics of upregulation of cyclin E and Skp2, a substrate-targeting subunit of the SCF ubiquitin ligase complex that regulates entry into S phase (Bashir et al., 2004). RAPL-deficient B and T cells exhibited comparable Skp2 upregulation and essentially the same time course of T187 phosphorylation (Figures 4A and 4C). The ratios of p27 phosphorylated on T187 to total p27 were lower in RAPL-deficient B cells (0.42 at 48 hr) and T cells (0.18 at 48 hr), compared to those of wild-type B cells (0.9 at

48 hr) and T cells (0.22 at 72 hr) (Figures 4A and 4C). The decreased phosphorylation on T187 of p27 might reflect cytoplasmic accumulation of p27 in RAPL-deficient lymphoblasts (Figure 3C; Figure S3), because T187 was mainly phosphorylated by Cdk2-cyclinE in the nucleus (Hara et al., 2001; Lee and Kay, 2007). These data suggest that RAPL deficiency does not affect T187 phosphorylation and Skp2-dependent proteolysis of p27 in the nucleus.

Serine 10 (S10), the major phosphorylation site of p27 (Ishida et al., 2000), is required for cytoplasmic localization at the G_0-G_1 transition in response to mitogenic stimulation (Rodier et al., 2001). S10 phosphorylation was high in resting wild-type B cells, declined to the lowest amounts at 2 and 12 hr poststimulation, and were subsequently undetectable as p27 was degraded (Figure 4A). Resting RAPL-deficient B cells showed similar amounts of S10 phosphorylation; however, S10 phosphorylation did not decrease at 2 and 12 hr poststimulation and were maintained in high amounts levels even at 72 hr (Figure 4A), as well as that of cytoplasmic p27 in B cell lymphoma (Figure 3D). We also examined S10 phosphorylation at early time points after stimulation. In wild-type B cells, S10 phosphorylation was decreased as early as 5 min after stimulation and further declined thereafter (Figure 4B). In contrast, S10 phosphorylation was relatively constant with a slight increase at 10 min in RAPL-deficient B cells (Figure 4B). There were no differences in Akt and Erk phosphorylation in wild-type and RAPL-deficient B cells (Figures 4B; Figure S2A), ruling out the involvement of these kinases in elevated S10 phosphorylation in RAPL-deficient B cells.

T cells showed different magnitudes and patterns of S10 phosphorylation compared to B cells. The S10 phosphorylation in resting T cells were lower than those in resting B cells. S10 phosphorylation was augmented at 12 and 24 hr poststimulation with anti-CD3+anti-CD28 (Figure 4C). RAPL-deficient T cells exhibited similar kinetics of S10 phosphorylation, with approximately 2-fold higher amounts (Figure 4C). When kinetic experiments were performed at early time points, S10 phosphorylation was transiently increased at 5–10 min and returned to basal levels 30 min after anti-CD3 and anti-CD28 stimulation (Figure 4D). RAPL-deficient T cells displayed similar, transient but enhanced S10 phosphorylation (Figure 4D). Stimulation with anti-CD3 alone induced S10 phosphorylation almost comparable to that by anti-CD3 and anti-CD28 (Figure S4A), indicating that phosphorylation of p27 at S10 is mainly regulated through TCR signaling. Thus, enhanced phosphorylation on S10 occurs at 5–10 min and 12–24 hr after stimulation in RAPL-deficient T cells, which precedes degradation of p27 and the entry to S phase. Again, there were no changes in Akt and Erk phosphorylation in RAPL-deficient T cells (Figure 4D; Figure S2A). Collectively, these results suggest that RAPL deficiency specifically upregulates S10 phosphorylation that is important for the cytoplasmic localization of p27 in lymphocytes.

Because IL-7 has been reported to stimulate proliferation through enhanced p27 destabilization in an IL-7-dependent thymocyte cell line (Li et al., 2006b), we examined the effect of IL-7 on S10 phosphorylation. IL-7 augmented proliferation of T cells from wild-type and RAPL-deficient mice to the same extent (approximately 4-fold) in the presence of anti-CD3 (Figure S4B). IL-7 did not affect S10 phosphorylation in both wild-type and RAPL-deficient T cells (Figure S4C), indicating that IL-7 enhanced proliferation independently of RAPL.

Mislocalization of p27 in the Cytoplasm of RAPL-Deficient Cells

We next examined p27 redistribution in primary lymphocytes by immunostaining. Unexpectedly, resting T and B lymphocytes exhibited distinct p27 distribution patterns: in B cells p27 was predominantly cytoplasmic (83.5% ± 3% of p27), but in T cells, the majority of p27 was localized in the nucleus (94.2% ± 1.2% of p27) (Figure 5A). Quantitative results showed that the distribution of p27 in the cytoplasm was essentially the same in resting wild-type and RAPL-deficient B cells (Figure 5B). Similar to wild-type T cells, most RAPL-deficient T cells also showed nuclear localization of p27 with a minor population showing cytoplasmic localization (Figure 5B).

After anti-BCR stimulation, p27 was dynamically redistributed in wild-type B cells. p27 rapidly clustered in the cytoplasm near the nucleus 20 min after stimulation and relocated into the nucleus at 2 hr (Figure 5C). Quantitative analysis showed that p27 distribution was predominantly nuclear in approximately 40% of the population at 2 hr (Figure 5D; Figure S5A). At 20 hr, the amount of p27 in the nucleus decreased with some remaining in the cytoplasm (Figure 5C; Figure S5B). In RAPL-deficient B cells, p27 also rapidly clustered in the cytoplasm (Figure 5C). However, in more than 80% of cells, p27 failed to localize to the nucleus at 2 hr and remained abundant in the cytoplasm at 20 hr (Figures 5C and 5D; Figure S5). Preferential decrease of p27 in the nucleus with residual p27 in the cytoplasm of wild-type B cells suggested that p27 degradation occurs mostly in the nucleus and that RAPL deficiency impaired a step in p27 nuclear translocation in B cells. The subcellular location of p27 is consistent with S10 phosphorylation kinetics and amounts.

Although a majority of p27 was present in the nucleus of resting wild-type T cells, a fraction of p27 was also cytoplasmic in most T cells 20 min after anti-CD3 and anti-CD28 stimulation, and 20% of the T cells exhibited the cytoplasmic-dominant distribution of p27 at 2 hr (Figures 5E and 5F). Meanwhile, the cytoplasmic-dominant population was almost doubled in RAPL-deficient T cells 2 hr and 20 hr after stimulation (Figures 5E and 5F). The similar increase in the cytoplasmic-dominant distribution was observed in RAPL-deficient T cells at 2 hr after stimulation with anti-CD3 alone (data not shown). Thus, these results indicate the possibility that RAPL modulates the cytoplasmic localization of p27 through S10 phosphorylation.

Inhibition of p27 S10 Phosphorylation and Enhanced Nuclear Localization by RAPL

To examine whether RAPL modulates S10 phosphorylation and subcellular localization of p27, we employed a heterologous system by using 293T cells, which are well characterized for nuclear export of p27 (Boehm et al., 2002; Ishida et al., 2002). S10 was basally phosphorylated in serum-starved 293T cells, increased at 0.5 hr after serum stimulation, and then peaked at 1–5 hr to amounts similar to that in continuously growing cells (Figure S6A). In contrast, in serum-starved RAPL-transfected 293T cells, basal and serum-induced S10 phosphorylation was severely diminished (Figure S6A). In loss-of-function mutant lacking the N-terminal half (RAPLΔN) (Katagiri et al., 2003)-transfected

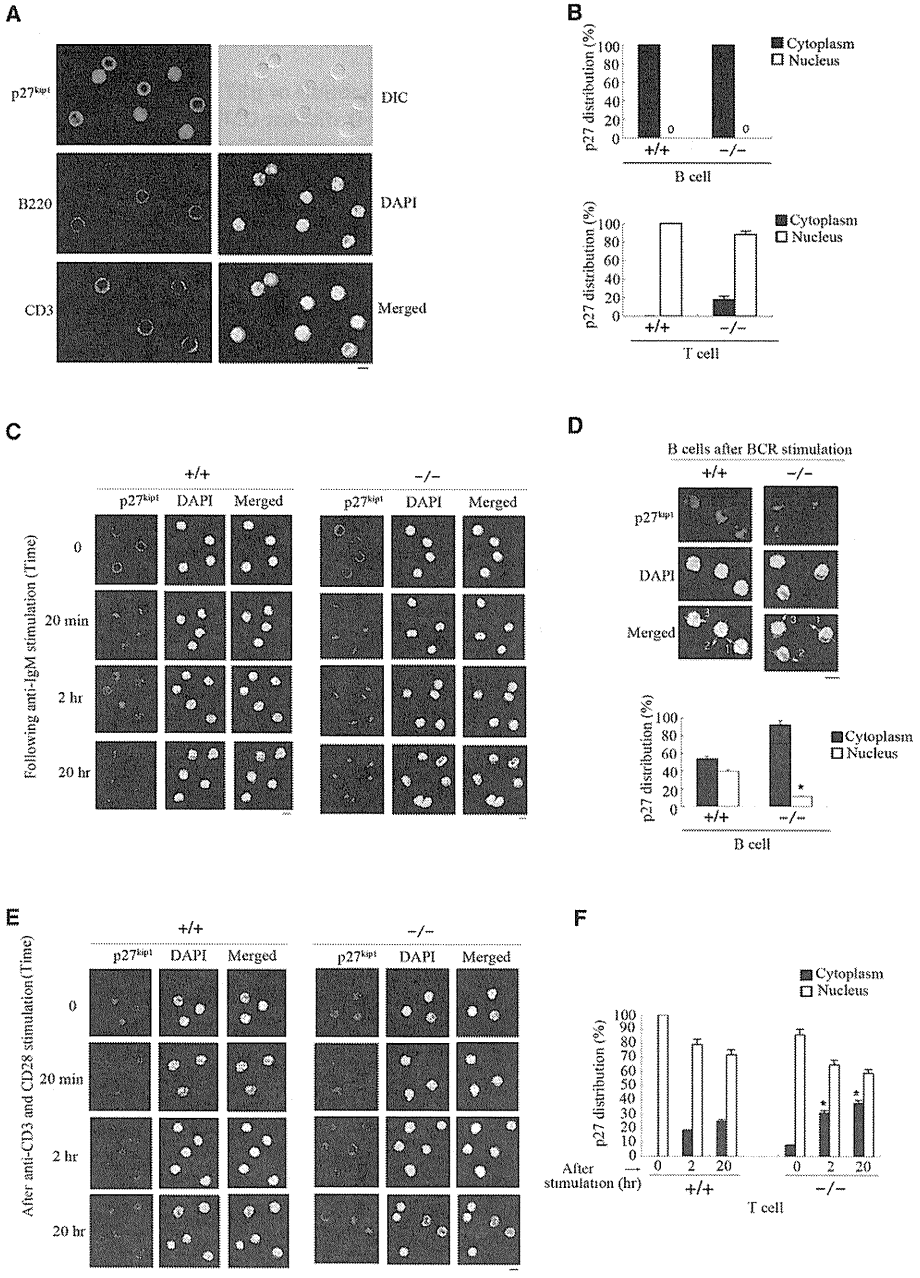

Figure 5. Impaired Redistribution of p27 in RAPL-Deficient B and T Lymphocytes after Antigen Receptor Stimulation

(A and B) Primary lymphocytes from the lymph nodes of wild-type (+/+) and RAPL-deficient (−/−) mice were stained for p27, B220, and CD3. The number of cells with a cytoplasmic and nuclear distribution p27 were visualized and counted by confocal microscopy. At least 100 cells were counted in different microscopic fields. Representative images of p27, B220, CD3, DIC, and DAPI in wild-type cells and average percentages and standard errors for three independent experiments are shown (B). Scale bar represents 5 μm.

(C) Redistribution of p27 in wild-type (+/+) (left) and RAPL-deficient (−/−) (right) B cells. Primary B cells were stimulated with anti-IgM for the indicated times and stained for p27 and nuclei (DAPI). Note that in wild-type B cells, cytoplasmic p27 was translocated into nuclei 2 hr after stimulation before degradation (left), but in RAPL-deficient B cells, cytoplasmic p27 failed to localize in nuclei (right). Scale bars represent 5 μm.

(D) High magnification of cytoplasmic and nuclear distribution of p27 in wild-type (+/+) and RAPL-deficient (−/−) B cells 2 hr after stimulation are shown. Line profiles of p27 and DAPI along the arrows are shown in Figure S5. The average percentages of cells showing nuclear- (open bar) or cytoplasmic- (closed bar) dominant p27 staining in three independent experiments are shown in the lower panel. A minimum of 100 cells were scored per treatment group. *$p < 0.001$, compared with corresponding wild-type littermate control. Scale bar represents 5 μm. The percentages of the nuclear fraction of p27 in the nuclear- and cytoplasmic-dominant population of wild-type B cells were 78.6% ± 6.9% and 36.1% ± 5.5%, and those of RAPL-deficient B cells were 58.5% ± 4.9% and 21.8% ± 2.4%. The difference in the percentages of nuclear p27 between nuclear- and cytoplasmic-dominant population was statistically significant ($p < 0.002$).

293T cells, serum-induced S10 phosphorylation was not decreased (Figure 6A). At 5 hr after serum addition, 51.2% ± 3.1% of p27 was cytoplasmic in control cells. Under the same conditions, 82.2% ± 7.4% of p27 was nuclear in RAPL-expressing cells with very low amounts in the cytoplasm, but this effect was not observed in RAPLΔN-expressing cells (Figure 6B), consistent with the S10 phosphorylation amounts of p27 (Figure 6A). RAPL, but not RAPLΔN expression, reduced the frequency of cells in S phase at 20 hr after serum stimulation (Figure 6C). This reduction was abrogated by p27 silencing (Figure 6D), indicating that the inhibitory effect of RAPL on proliferation depends on p27.

We also confirmed the similar effects of RAPL on p27 localization by using CH27 B cell lymphoma cells. RAPL expression promoted nuclear localization and significantly decreased cell proliferation (Figure S6B). This suppressive effect of RAPL on proliferation was also abrogated by p27 silencing (Figure S6B).

If RAPL could promote nuclear localization of p27 through suppression of S10 phosphorylation, cytoplasmic localization of a phosphomimetic mutant p27S10D (Ishida et al., 2000) should not be affected by RAPL. To examine this possibility, Flag-tagged p27 and p27S10D were transfected into control and RAPL-expressing cells. The cells were synchronized by serum starvation, then added to serum for 6 hr before staining. Wild-type p27 was localized in the cytoplasm of control cells, whereas it was mainly present in the nucleus of RAPL-expressing cells, as is the case with endogenous p27 (Figure 6E). In contrast, approximately 90% of p27S10D was localized in the cytoplasm of both control and RAPL-expressing cells (Figure 6E), indicating that S10D is dominant over RAPL for p27 localization. This provides further support for the notion that RAPL regulates p27 localization through suppression of S10 phosphorylation.

Because kinase interacting stathmin (KIS) was reported to phosphorylate S10 in the G1 phase (Boehm et al., 2002), we investigated whether RAPL could inhibit KIS kinase activity. The Flag-tagged mouse KIS and RAPL were cotransfected into 293 T cells, and we examined immune-complex kinase activity of KIS by using p27 and p27S10A protein as a substrate. KIS phosphorylated the wild-type p27 but not the p27 mutant in which serine 10 is substituted with alanine (p27S10A) (Figure S6C), as reported (Boehm et al., 2002). RAPL expression reduced the kinase activity of KIS on S10 by 60% (Figure S6C). Meanwhile, silencing of KIS in 293T cells increased nuclear-dominant localization of p27, as previously reported (Boehm et al., 2002), and RAPL overexpression had marginal effects on the nuclear localization of p27 in KIS-silenced 293T cells (data not sown). This result suggests that RAPL could decrease the phosphorylation of p27 on S10 at least through the suppression of KIS activity.

The S10A Mutation in p27^{kip1} Suppresses Autoimmunity and B Cell Lymphoma in RAPL-Deficient Mice

If the growth stimulatory effect of RAPL deficiency is mediated by S10 phosphorylation of p27, it would be expected that the S10A mutation could counteract its effect and prevent lymphoproliferative diseases of RAPL-deficient mice. To examine this possibility, we crossed p27S10A genetically targeted mice (Kotake et al., 2005) with RAPL-deficient mice to generate *Cdkn1b*$^{S10A/S10A}$ RAPL-deficient mice (Figure 7A). As shown in Figure 7B, the S10A mutation in p27 significantly reduced the CD138^{+}B220^{+} plasma cells by 67% and CD44^{+}CD62L^{-} effector-memory T cells by 28%. Accordingly, the titers of antibodies to double-stranded DNA (dsDNA) decreased by 58%, the incidence of proteinuria was reduced (63% versus 22%), and also deposition of IgG was rarely detected (Figure 7C; Figure S7A), indicating that the S10A mutation suppressed the development of severe glomerulonephritis in 10-month-old RAPL-deficient mice. Importantly, B cell lymphoma and other tumors did not develop in *Cdkn1b*$^{S10A/S10A}$ RAPL-deficient mice (Figure 7D; Figure S7B).

In resting *Cdkn1b*$^{S10A/S10A}$ B cells sufficient or deficient for RAPL, p27 was mainly located in the cytoplasm as seen in the wild-type situation, although its distribution tended to be aggregated near the nucleus (Figure 7E). In *Cdkn1b*$^{+/+}$ RAPL-deficient B cells, p27 remained in the cytoplasm after stimulation (Figure 5C). In contrast, when *Cdkn1b*$^{S10A/S10A}$ RAPL-deficient B cells were stimulated with anti-IgM, p27S10A translocated into the nucleus in both RAPL-sufficient and -deficient B cells with comparable numbers of cells showing nuclear-dominant p27 (Figure 7E; Figure S7C). p27 degradation in *Cdkn1b*$^{S10A/S10A}$ RAPL-deficient B cells was greatly accelerated compared to that of *Cdkn1b*$^{+/+}$ RAPL-deficient B cells (Figure S7D), and the level of degradation was almost equivalent to that of wild-type B cells (Figure 3B). *Cdkn1b*$^{S10A/S10A}$ RAPL-deficient B cells did not exhibit enhanced proliferation with anti-IgM, compared to those of *Cdkn1b*$^{S10A/S10A}$ RAPL-sufficient B cells and wild-type B cells (Figure 7E). Thus, S10A mutation corrected B cell abnormalities.

In *Cdkn1b*$^{S10A/S10A}$ T cells sufficient or deficient for RAPL, p27 was mainly located in the nucleus, as is the case with *Cdkn1b*$^{+/+}$ T cells (Figure 7F). When stimulated with anti-CD3 and anti-CD28, the proportion of the cells expressing p27S10A translocated into the cytoplasm was lower than that of the cells with wild-type p27 (21.4% versus 33.1%) (Figure 7F; Figure S7C). There was no significant increase of RAPL-deficient T cells with cytoplasmic-dominant localization of p27S10A (20.6%) (Figure 7F; Figure S7C). p27 degradation in *Cdkn1b*$^{S10A/S10A}$ RAPL-deficient T cells was also enhanced compared to that of *Cdkn1b*$^{+/+}$ RAPL-deficient T cells (Figure S7D), and the amount

(E) Redistribution of p27 in wild-type (+/+) (left) and RAPL-deficient (right) T cells. Primary T cells were stimulated with anti-CD3 and anti-CD28 for the indicated times and stained for p27 and nuclei (DAPI), as in (C). Note that a portion of nuclear p27 was translocated into the cytoplasm after stimulation in both wild-type and RAPL-deficient T cells, but cells showing predominantly cytoplasmic p27 increased in RAPL-deficient T cells compared with wild-type T cells. Scale bar represents 5 μm.

(F) The average percentages of cells showing nuclear- (open bar) or cytoplasmic- (closed bar) dominant p27 in three independent experiments are shown. Wild-type (+/+) and RAPL-deficient T cells were stimulated for 2 hr or 20 hr with anti-CD3+anti-CD28. A minimum of 100 cells were scored per treatment group. *$p < 0.005$, compared with corresponding wild-type littermate control. The percentages of cytoplasmic p27 in the cytoplasmic and nuclear-dominant population of wild-type T cells were 62.5% ± 5.6% and 17.9% ± 11.3%, and those of RAPL-deficient T cells were 66.1% ± 6.0% and 25.6% ± 15.2%. The difference in the percentages of cytoplasmic p27 between cytoplasmic- and nuclear-dominant population was statistically significant ($p < 0.001$).

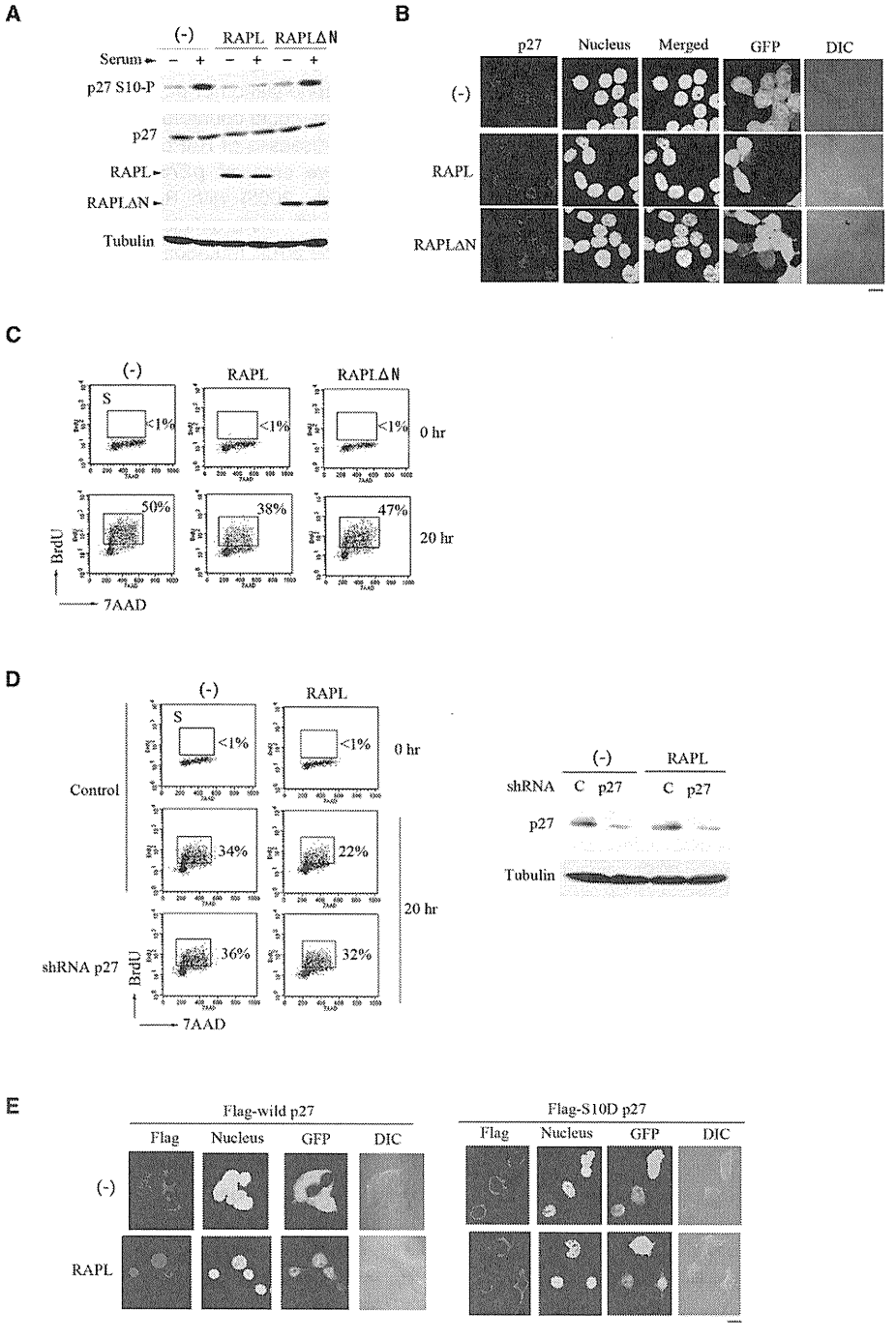

Figure 6. RAPL Promotes p27 Nuclear Localization and Suppresses S Phase Entry

(A) RAPL mutant did not inhibit p27 phosphorylation on S10. 293T cells with or without RAPL or RAPLΔN expression were serum starved for 2 days and then stimulated with 10% serum for 5 hr. Total and S10 phosphorylated p27, myc-RAPL or myc-RAPLΔN, and tubulin are shown. Total lysates derived from 1×10^4 cells were applied in each lane.

(B) Inhibition of p27 nuclear export by RAPL but not RAPLΔN. 293T cells were transfected with GFP alone (–), RAPL, or RAPLΔN plus GFP (green) and then stimulated with serum for 5 hr after serum starvation for 2 days. Cells were immunostained for p27 (red) and DAPI (nuclei). Scale bar represents 10 μm.

(C) Cell cycle analysis of 293T cells without (–) or with RAPL or RAPLΔN expression before or after serum stimulation for 20 hr. The percentage of cells labeled with BrdU (S phase) is shown in each panel. The results are representative of three independent experiments.

(D) Cell cycle analysis of control or p27-specific shRNA transfected 293T cells without (–) or with RAPL expression before or after serum stimulation for 20 hr. The percentage of cells labeled with BrdU (S phase) is shown in each panel. The results are representative of three independent experiments

of downregulation was almost equal to that of wild-type T cells (Figure 3B). The cytoplasmic mislocalization of p27 in *Cdkn1b*$^{+/+}$ RAPL-deficient T cells with anti-CD3 was also corrected with S10A mutation on p27 (Figure S7E). These results indicate that the mislocalization and degradation of p27 in RAPL-deficient T cells was dependent on S10 phosphorylation. T cells from *Cdkn1b*$^{S10A/S10A}$ RAPL-deficient T cells exhibited lower proliferation compared to *Cdkn1b*$^{+/+}$ RAPL-deficient T cells, but it was still significantly higher than *Cdkn1b*$^{S10A/S10A}$ RAPL-sufficient T cells (Figure 7F). These data suggest that hyperproliferation of T cells by RAPL deficiency was partly dependent on S10 phosphorylation, although other mechanisms are probably involved.

All together, these results demonstrate that RAPL-dependent regulation of phosphorylation of p27 on S10 plays important roles for prevention of lupus-like glomerulonephritis and B cell lymphoma.

DISCUSSION

Our results demonstrated a role for RAPL in suppression of S10 phosphorylation of p27 and nuclear export of p27, thereby retarding the G1-S phase transition. The defective checkpoint in the G1-S transition resulting from RAPL deficiency enhanced proliferation, leading to lupus-type glomerulonephritis and lymphomas. p27S10A genetic targeting in the RAPL-deficient background rescued both glomerulonephritis and B cell lymphoma and demonstrates that S10 phosphorylation of p27 is critical for the development of lymphoproliferative diseases by RAPL deficiency.

Our results suggest that mislocalized p27 leads to increased Cdk2 activity, which in turn promotes G1-S phase transition in lymphocytes. It was reported that Cdc2 plays a role in S-phase entry in the absence of Cdk2 (Aleem et al., 2005). p27 also associates with and inhibits Cdc2 (Aleem et al., 2005). The experiment with a Cdk2 inhibitor favors the major role of Cdk2 in S phase entry of normal lymphocytes, although prolonged Cdk2 deficiency might lead to compensation with Cdc2. In either case, it is possible that RAPL suppresses both Cdk2 and Cdc2 activity through the promotion of p27 nuclear localization and regulates S phase entry of lymphocytes after stimulation through antigen receptors.

The S10 mutation of p27 completely abrogated the hyperproliferative responses of RAPL-deficient B cells, but partially inhibited those of RAPL-deficient T cells, indicating that other mechanisms operate in RAPL-deficient T cells. Mst1 is activated by Rap1 and RAPL and responsible for Rap1- and RAPL-dependent integrin regulation (Katagiri et al., 2006, 2009). Mst1 is also involved in T cell proliferation (Avruch et al., 2009; Katagiri et al., 2009). Proliferative responses were augmented in *Mst1*$^{-/-}$ T cells, but not B cells (Avruch et al., 2009; Katagiri et al., 2009). However, p27 regulation in *Mst1*$^{-/-}$ lymphocytes was found to be normal (unpublished data). Thus, Mst1 differently regulates lymphocyte proliferation independently of p27, and hyperproliferative responses observed in *Cdkn1b*$^{S10A/S10A}$ RAPL-deficient T cells might be due to defective activation of Mst1 by RAPL deficiency.

This study shows that KIS appears to be a relevant target of RAPL during the G1-S transition, because KIS phosphorylates S10 during the G1 phase in response to mitogenic stimulation and promotes its nuclear export (Boehm et al., 2002). Interestingly, KIS was reported to play important roles in cell cycle progression of leukemia cell lines through the promotion of S10 phosphorylation of p27 (Nakamura et al., 2008), suggesting an important role of KIS in lymphoid cells. However, multiple kinases besides KIS were also reported to phosphorylate p27 at S10 including Cdk5 (Kawauchi et al., 2006), suggesting a complex network of redundant kinases controlling p27 degradation and cell cycle progression in vivo. It will be important to examine whether RAPL could regulate KIS and other kinase activities in lymphocytes.

The importance of RAPL regulation in the cell cycle is supported by the incidence of lupus-like glomerulonephritis disease. Although RAPL-deficient mice are lymphopenic at a young age, both RAPL-deficient T and B cells are activated and differentiate into effector-memory T cells and plasma cells with age. In a lymphopenic state, self-antigens provide proliferation-inducing signals that expand T cells until the T cell pool is reestablished to a nearly normal size (Lawson et al., 2001). It is conceivable that a lymphopenic state resulting from defective lymphocyte trafficking in RAPL-deficient mice favors homeostatic proliferation of self-reactive clones, which predisposes mice to autoimmune disease. IL-7 is critical for homeostatic proliferation together with signals from the TCR recognizing a complex of self-peptides and MHC (Jacobs et al., 2010; Tan et al., 2001). IL-7 might help expanding self-reactive clones in RAPL-deficient mice.

Enhanced lymphocyte proliferation probably increases the development of spontaneous B cell lymphomas in RAPL-deficient mice. RAPL-deficient mice also developed lung and liver tumors after 1.5 yr of age, suggesting a tumor-suppressor function for RAPL in nonlymphoid organs, despite low RAPL expression in these tissues. There are several studies showing that cytoplasmic p27 is associated with hyperproliferation and tumorigenesis through a cyclin-Cdk-independent function (Besson et al., 2006, 2007). Cytoplasmic mislocalization of p27 might underlie the development of spontaneous tumors in RAPL-deficient mice. It was also reported that the *NORE1B* (*RASSF5C*) gene was frequently inactivated in human hepatocellular carcinomas because of promoter methylation (Macheiner et al., 2006). It will be interesting to study involvement of downregulation of RAPL in human hyperproliferative autoimmune and malignant diseases.

Our findings that RAPL, a molecule originally identified as an integrin regulator, also plays an inhibitory role in cell proliferation provides a molecular link with cell adhesion and growth. In line with this notion, a constitutively active LFA-1 was found to be rather inhibitory to antigen-induced proliferation (Semmrich et al., 2005). Rap1 and p27 were previously reported to be

(left). Immunoblot of p27 and tubulin in RAPL or vector control (–) expressing 293T cell lysates after control-(c) or p27-specific (p27) shRNA transfection (right).

(E) A S10D mutation of p27 inhibited the nuclear localization of p27 by RAPL. 293T cells were transfected with flag-tagged wild-type or S10D mutant p27 together with GFP alone (–) or RAPL plus GFP (green), and then stimulated with serum for 5 hr after serum starvation for 2 days. Cells were immunostained for flag (red) and DAPI (nuclei). Scale bar represents 10 μm.

Please cite this article in press as: Katagiri et al., Deficiency of Rap1-Binding Protein RAPL Causes Lymphoproliferative Disorders through Mislocalization of p27kip1, Immunity (2011), doi:10.1016/j.immuni.2010.12.010

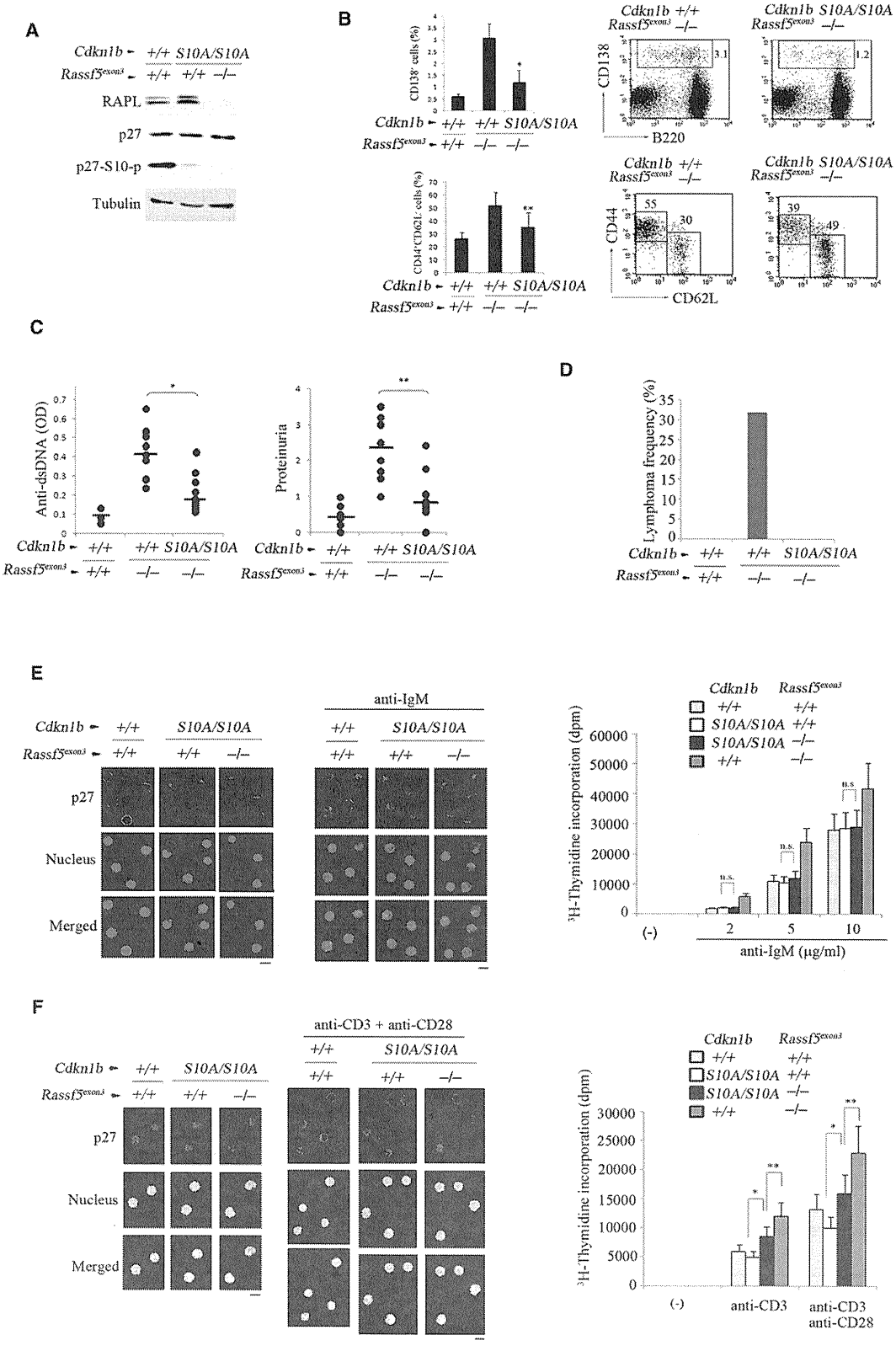

involved in T cell anergy (Boussiotis et al., 2000). Recent studies suggest that cytoplasmic p27 can inhibit cell migration behaviors by binding to Rho or stathmin (Baldassarre et al., 2005). Further characterization of these processes will facilitate our understanding on the link between cell adhesion and proliferation thorough RAPL. Our studies provide important clues and experimental systems to elucidate how disruption of coordinated regulation of adhesion and proliferation leads to autoimmunity and carcinogenesis.

EXPERIMENTAL PROCEDURES

Plasmids, antibodies, and reagents are described in Supplemental Experimental Procedures.

Mice

RAPL-deficient mice were generated by targeting the RAPL-specific exon3 of *Rassf5* as previously described (Katagiri et al., 2004). Homozygous mice and littermate control mice were crossed with wild-type C57BL/6 mice for eight generations. Mice were housed in specific-pathogen-free conditions and all experiments were in accordance with protocols approved by the Animal Care and Use Committee of Kansai Medical University (Osaka, Japan). p27 genetically targeted mice harboring an S10A mutation were generated as previously described (Kotake et al., 2005).

Immunoprecipitation, Immunoblot, and In Vitro Kinase Assays

Immunoprecipitation and immunoblot were performed as described in Supplemental Experimental Procedures. Signals of appropriate bands were quantified with an image analyzer (BAS-1500, Fujifilm). Kinase assays for Cdk2 and Cdk4 were performed as described before (Nakayama et al., 1996). In brief, immunoprecipitates with rabbit anti-Cdk2 or anti-Cdk4 from cell lysates from T or B cells stimulated with anti-IgM $(Fab')_2$ or anti-CD3 and anti-CD28 were washed with lysis buffer (Nonidet P-40, 150 mM NaCl, 25 mM Tris-HCl [pH 7.4], 10% glycerol) and suspended in 30 μl of kinase buffer (50 mM HEPES [pH 7.4], 10 mM $MgCl_2$, 1 mM DTT, 10 mM β-glycerophosphate) containing 1 μg Histone H1 (Calbiochem) or 0.5 μg GST-Rb (Santa-Cruz) and 25 μM ATP, 10 μCi [γ-^{32}P]ATP (6000 Ci/mmol, Amersham). The samples were incubated at 30°C for 30 min, denatured in SDS sample buffer, and run on a 15% SDS-polyacrylamide gel (Nakayama et al., 1996). Kinase assays of KIS were done with GST-p27 and GST-p27S10A, as described (Boehm et al., 2002). The signals from appropriate bands were quantified with a phosphoimager (BAS3000, Fujifilm) and fold-increase was calculated after background subtraction.

Immunostaining

Immunostaining procedures are described in Supplemental Experimental Procedures. Confocal images were obtained with a LSM510 META microscope with a 63× objective lens. Line profiles of cells stained for p27 and nuclei (DAPI) were used to measure nuclear/cytoplasmic p27 distribution (see Supplemental Experimental Procedures and Figure S3 for details). Cell surface staining and analysis with a FACSCalibur (Beckton-Dickinson) flow cytometer were previously described (Katagiri et al., 2004). For immunohistochemistry of kidney tissues to detect IgG and C3 deposition, paraffin sections were dewaxed, blocked with diluted horse serum, and then stained with FITC-goat anti-mouse IgG and C3.

Cell Proliferation and BrdU Incorporation Assays

B and T lymphocytes purified from spleens or lymph nodes were cultured at 1.5 × 10^5/ml in 0.2 ml per well of a 96-well plate with or without anti-IgM $F(ab')_2$ or anti-CD3(5 μg/ml and CD28 (2 μg/ml) for 48 hr. [^{3}H]-thymidine (1 μmCi/well) was added for the last 6 hr. Cells were harvested and [^{3}H]-thymidine uptake was measured. To determine the frequency and nature of individual cells that synthesized DNA during culture, BrdU incorporation was performed with a BrdU flow kit according to the manufacturer's instruction (BD PharMingen). BrdU uptake in vivo is described in Supplemental Experimental Procedures.

Statistical Analysis

Student's two-tailed t test was used to compare experimental groups. p values less than 0.05 were considered significant.

SUPPLEMENTAL INFORMATION

Supplemental Information includes Supplemental Experimental Procedures and seven figures and can be found with this article online at doi:10.1016/j.immuni.2010.12.010.

ACKNOWLEDGMENTS

We would like to thank S. Matsuda (Kansai Medical University, Japan) for critical reading of the manuscript and S. Ohishi, K. Maebara, and R. Hamaguchi for technical assistance. This research was supported by grants-in-aid from the Ministry of Education, Culture, Sports, Science and Technology of Japan and the Ministry of Health, Labor and Welfare, and from CREST Japan

Figure 7. Effects of S10A Mutation on RAPL-Deficient Mice

(A) Expression of RAPL, p27, phospho-S10 of p27, and tubulin in B cells derived from *Cdkn1b*$^{+/+}$*Rassf5*$^{exon3+/exon3+}$, *Cdkn1b*$^{S10A/S10A}$*Rassf5*$^{exon3+/exon3+}$, and *Cdkn1b*$^{S10A/S10A}$*Rassf5*$^{exon3-/exon3-}$ mice.

(B) The ratios of CD138$^+$ and B220$^+$ lymphocytes (top left) or CD44$^+$ and CD62L$^-$ on CD4$^+$ gated lymphocytes (bottom left) from spleens of *Cdkn1b*$^{+/+}$*Rassf5*$^{exon3+/exon3+}$, *Cdkn1b*$^{+/+}$*Rassf5*$^{exon3-/exon3-}$, and *Cdkn1b*$^{S10A/S10A}$*Rassf5*$^{exon3-/exon3-}$ mice at 10 months of age. Flow cytometric profiles of expression of CD138 and B220 (top right) and CD44 and CD62L on CD4$^+$ gated lymphocytes (bottom right). *p < 0.02, **p < 0.05.

(C) Anti-double-strand DNA titers in 12-month-old *Cdkn1b*$^{+/+}$*Rassf5*$^{exon3+/exon3+}$, *Cdkn1b*$^{+/+}$*Rassf5*$^{exon3-/exon3-}$, and *Cdkn1b*$^{S10A/S10A}$*Rassf5*$^{exon3-/exon3-}$ (left). Proteinuria in 12-month-old mice (right). Proteinuria was measured with medical color strips. p values for *Cdkn1b*$^{S10A/S10}$*Rassf5*$^{exon3-/exon3-}$ mice compared to *Cdkn1b*$^{+/+}$*Rassf5*$^{exon3-/exon3-}$ mice are indicated on the graph. *p < 0.02, **p < 0.01.

(D) Development of B cell lymphomas in *Cdkn1b*$^{+/+}$*Rassf5*$^{exon3+/exon3+}$, *Cdkn1b*$^{+/+}$*Rassf5*$^{exon3-/exon3-}$, and *Cdkn1b*$^{S10A/S10A}$*Rassf5*$^{exon3-/exon3-}$ mice at 12 months of age. Lymph nodes and spleens from 20 mice per each group were subjected for histological examination.

(E) Left: The S10A mutation abrogated mislocalization of p27 with anti-IgM $F(ab')_2$. Redistribution of p27 in B cells from *Cdkn1b*$^{+/+}$*Rassf5*$^{exon3+/exon3+}$, *Cdkn1b*$^{S10A/S10A}$*Rassf5*$^{exon3+/exon3+}$, and *Cdkn1b*$^{S10A/S10A}$*Rassf5*$^{exon3-/exon3-}$ mice. Primary B cells were stimulated with anti-IgM $F(ab')^2$ for 2 hr and stained for p27 and nuclei (DAPI). Scale bars represent 5 μm. Right: The S10A mutation abrogated hyperproliferation of RAPL-deficient B cells with anti-IgM $F(ab')_2$. [^{3}H]-thymidine uptake by B cells. Primary B from *Cdkn1b*$^{+/+}$*Rassf5*$^{exon3+/exon3+}$, *Cdkn1b*$^{S10A/S10A}$*Rassf5*$^{exon3+exon3/+}$, *Cdkn1b*$^{S10A/S10A}$*Rassf5*$^{exon3-/exon3-}$, and *Cdkn1b*$^{+/+}$*Rassf5*$^{exon3-/exon3-}$ mice were unstimulated (–) or stimulated with anti-IgM $F(ab')_2$ at concentrations indicated.

(F) Left: The S10A mutation corrected mislocalization of p27 with anti-CD3 and anti-CD28. Redistribution of p27 in T cells from *Cdkn1b*$^{+/+}$*Rassf5*$^{exon3+/exon3+}$, *Cdkn1b*$^{S10A/S10A}$*Rassf5*$^{exon3+/exon3+}$, and *Cdkn1b*$^{S10A/S10A}$*Rassf5*$^{exon3-/exon3-}$ mice. Primary T cells were stimulated with anti-CD3 and anti-CD28 for 2 hr and stained for p27 and nuclei (DAPI). Scale bars represent 5 μm. Right: The S10A mutation decreased hyperproliferative responses of RAPL-deficient T cells with anti-CD3 and anti-CD3+CD28. [^{3}H]-thymidine uptake by T cells. Primary T from *Cdkn1b*$^{+/+}$*Rassf5*$^{exon3+/exon3+}$, *Cdkn1b*$^{S10A/S10A}$*Rassf5*$^{exon3+/exon3+}$, *Cdkn1b*$^{S10A/S10A}$*Rassf5*$^{exon3-/exon3-}$, and *Cdkn1b*$^{+/+}$*Rassf5*$^{exon3-/exon3-}$ mice were unstimulated (–) or stimulated with anti-CD3 and anti-CD3$^+$CD28. *p < 0.01, **p < 0.03.

Science and Technology Agency, and research grants from Takeda Science Foundation, Yasuda Medical foundation, Japan Leukemia Research Fund, and Astellas Foundation for Research on Metabolic Disorders.

Received: May 11, 2010
Revised: September 25, 2010
Accepted: December 15, 2010
Published online: December 30, 2010

REFERENCES

Aleem, E., Kiyokawa, H., and Kaldis, P. (2005). Cdc2-cyclin E complexes regulate the G1/S phase transition. Nat. Cell Biol. *7*, 831–836.

Appleman, L.J., Berezovskaya, A., Grass, I., and Boussiotis, V.A. (2000). CD28 costimulation mediates T cell expansion via IL-2-independent and IL-2-dependent regulation of cell cycle progression. J. Immunol. *164*, 144–151.

Avruch, J., Xavier, R., Bardeesy, N., Zhang, X.F., Praskova, M., Zhou, D., and Xia, F. (2009). Rassf family of tumor suppressor polypeptides. J. Biol. Chem. *284*, 11001–11005.

Baldassarre, G., Belletti, B., Nicoloso, M.S., Schiappacassi, M., Vecchione, A., Spessotto, P., Morrione, A., Canzonieri, V., and Colombatti, A. (2005). p27 (Kip1)-stathmin interaction influences sarcoma cell migration and invasion. Cancer Cell *7*, 51–63.

Balomenos, D., and Martinez, A.C. (2000). Cell-cycle regulation in immunity, tolerance and autoimmunity. Immunol. Today *21*, 551–555.

Barnouin, K., Fredersdorf, S., Eddaoudi, A., Mittnacht, S., Pan, L.X., Du, M.Q., and Lu, X. (1999). Antiproliferative function of p27kip1 is frequently inhibited in highly malignant Burkitt's lymphoma cells. Oncogene *18*, 6388–6397.

Bashir, T., Dorrello, N.V., Amador, V., Guardavaccaro, D., and Pagano, M. (2004). Control of the SCF(Skp2-Cks1) ubiquitin ligase by the APC/C(Cdh1) ubiquitin ligase. Nature *428*, 190–193.

Besson, A., Gurian-West, M., Chen, X., Kelly-Spratt, K.S., Kemp, C.J., and Roberts, J.M. (2006). A pathway in quiescent cells that controls p27Kip1 stability, subcellular localization, and tumor suppression. Genes Dev. *20*, 47–64.

Besson, A., Hwang, H.C., Cicero, S., Donovan, S.L., Gurian-West, M., Johnson, D., Clurman, B.E., Dyer, M.A., and Roberts, J.M. (2007). Discovery of an oncogenic activity in p27Kip1 that causes stem cell expansion and a multiple tumor phenotype. Genes Dev. *21*, 1731–1746.

Bhattacharjee, R.N., Banks, G.C., Trotter, K.W., Lee, H.L., and Archer, T.K. (2001). Histone H1 phosphorylation by Cdk2 selectively modulates mouse mammary tumor virus transcription through chromatin remodeling. Mol. Cell. Biol. *21*, 5417–5425.

Boehm, M., Yoshimoto, T., Crook, M.F., Nallamshetty, S., True, A., Nabel, G.J., and Nabel, E.G. (2002). A growth factor-dependent nuclear kinase phosphorylates p27(Kip1) and regulates cell cycle progression. EMBO J. *21*, 3390–3401.

Bos, J.L., de Rooij, J., and Reedquist, K.A. (2001). Rap1 signaling: Adhering to new models. Nat. Rev. Mol. Cell Biol. *2*, 369–377.

Boussiotis, V.A., Freeman, G.J., Taylor, P.A., Berezovskaya, A., Grass, I., Blazar, B.R., and Nadler, L.M. (2000). p27kip1 functions as an anergy factor inhibiting interleukin 2 transcription and clonal expansion of alloreactive human and mouse helper T lymphocytes. Nat. Med. *6*, 290–297.

Ebisuno, Y., Katagiri, K., Katakai, T., Ueda, Y., Nemoto, T., Inada, H., Nabekura, J., Okada, T., Kannagi, R., Tanaka, T., et al. (2010). Rap1 controls lymphocyte adhesion cascade and interstitial migration within lymph nodes in RAPL-dependent and -independent manners. Blood *115*, 804–814.

Ekholm, S.V., and Reed, S.I. (2000). Regulation of G(1) cyclin-dependent kinases in the mammalian cell cycle. Curr. Opin. Cell Biol. *12*, 676–684.

Fero, M.L., Rivkin, M., Tasch, M., Porter, P., Carow, C.E., Firpo, E., Polyak, K., Tsai, L.H., Broudy, V., Perlmutter, R.M., et al. (1996). A syndrome of multiorgan hyperplasia with features of gigantism, tumorigenesis, and female sterility in p27(Kip1)-deficient mice. Cell *85*, 733–744.

Hara, T., Kamura, T., Nakayama, K., Oshikawa, K., and Hatakeyama, S. (2001). Degradation of p27(Kip1) at the G(0)-G(1) transition mediated by a Skp2-independent ubiquitination pathway. J. Biol. Chem. *276*, 48937–48943.

Ishida, N., Kitagawa, M., Hatakeyama, S., and Nakayama, K. (2000). Phosphorylation at serine 10, a major phosphorylation site of p27(Kip1), increases its protein stability. J. Biol. Chem. *275*, 25146–25154.

Ishida, N., Hara, T., Kamura, T., Yoshida, M., Nakayama, K., and Nakayama, K.I. (2002). Phosphorylation of p27Kip1 on serine 10 is required for its binding to CRM1 and nuclear export. J. Biol. Chem. *277*, 14355–14358.

Jacobs, S.R., Michalek, R.D., and Rathmell, J.C. (2010). IL-7 is essential for homeostatic control of T cell metabolism in vivo. J. Immunol. *184*, 3461–3469.

Katagiri, K., Maeda, A., Shimonaka, M., and Kinashi, T. (2003). RAPL, a Rap1-binding molecule that mediates Rap1-induced adhesion through spatial regulation of LFA-1. Nat. Immunol. *4*, 741–748.

Katagiri, K., Ohnishi, N., Kabashima, K., Iyoda, T., Takeda, N., Shinkai, Y., Inaba, K., and Kinashi, T. (2004). Crucial functions of the Rap1 effector molecule RAPL in lymphocyte and dendritic cell trafficking. Nat. Immunol. *5*, 1045–1051.

Katagiri, K., Imamura, M., and Kinashi, T. (2006). Spatiotemporal regulation of the kinase Mst1 by binding protein RAPL is critical for lymphocyte polarity and adhesion. Nat. Immunol. *7*, 919–928.

Katagiri, K., Katakai, T., Ebisuno, Y., Ueda, Y., Okada, T., and Kinashi, T. (2009). Mst1 controls lymphocyte trafficking and interstitial motility within lymph nodes. EMBO J. *28*, 1319–1331.

Kawauchi, T., Chihama, K., Nabeshima, Y., and Hoshino, M. (2006). Cdk5 phosphorylates and stabilizes p27kip1 contributing to actin organization and cortical neuronal migration. Nat. Cell Biol. *8*, 17–26.

Kotake, Y., Nakayama, K., Ishida, N., and Nakayama, K.I. (2005). Role of serine 10 phosphorylation in p27 stabilization revealed by analysis of p27 knock-in mice harboring a serine 10 mutation. J. Biol. Chem. *280*, 1095–1102.

Lawson, B.R., Koundouris, S.I., Barnhouse, M., Dummer, W., Baccala, R., Kono, D.H., and Theofilopoulos, A.N. (2001). The role of alpha beta+ T cells and homeostatic T cell proliferation in Y-chromosome-associated murine lupus. J. Immunol. *167*, 2354–2360.

Lee, J.G., and Kay, E.P. (2007). Two populations of p27 use differential kinetics to phosphorylate Ser-10 and Thr-187 via phosphatidylinositol 3-Kinase in response to fibroblast growth factor-2 stimulation. J. Biol. Chem. *282*, 6444–6454.

Li, L., Iwamoto, Y., Berezovskaya, A., and Boussiotis, V.A. (2006a). A pathway regulated by cell cycle inhibitor p27Kip1 and checkpoint inhibitor Smad3 is involved in the induction of T cell tolerance. Nat. Immunol. *7*, 1157–1165.

Li, W.Q., Jiang, Q., Aleem, E., Kaldis, P., Khaled, A.R., and Durum, S.K. (2006b). IL-7 promotes T cell proliferation through destabilization of p27Kip1. J. Exp. Med. *203*, 573–582.

Macheiner, D., Heller, G., Kappel, S., Bichler, C., Stattner, S., Ziegler, B., Kandioler, D., Wrba, F., Schulte-Hermann, R., Zochbauer-Muller, S., and Grasl-Kraupp, B. (2006). NORE1B, a candidate tumor suppressor, is epigenetically silenced in human hepatocellular carcinoma. J. Hepatol. *45*, 81–89.

Nakamura, S., Okinaka, K., Hirano, I., Ono, T., Sugimoto, Y., Shigeno, K., Fujisawa, S., Shinjo, K., and Ohnishi, K. (2008). KIS induces proliferation and the cell cycle progression through the phosphorylation of p27Kip1 in leukemia cells. Leuk. Res. *32*, 1358–1365.

Nakayama, K., Ishida, N., Shirane, M., Inomata, A., Inoue, T., Shishido, N., Horii, I., and Loh, D.Y. (1996). Mice lacking p27(Kip1) display increased body size, multiple organ hyperplasia, retinal dysplasia, and pituitary tumors. Cell *85*, 707–720.

Polyak, K., Lee, M.H., Erdjument-Bromage, H., Koff, A., Roberts, J.M., Tempst, P., and Massague, J. (1994). Cloning of p27Kip1, a cyclin-dependent kinase inhibitor and a potential mediator of extracellular antimitogenic signals. Cell *78*, 59–66.

Qi, C.F., Xiang, S., Shin, M.S., Hao, X., Lee, C.H., Zhou, J.X., Torrey, T.A., Hartley, J.W., Fredrickson, T.N., and Morse, H.C., 3rd. (2006). Expression of the cyclin-dependent kinase inhibitor p27 and its deregulation in mouse B cell lymphomas. Leuk. Res. *30*, 153–163.

Please cite this article in press as: Katagiri et al., Deficiency of Rap1-Binding Protein RAPL Causes Lymphoproliferative Disorders through Mislocalization of p27kip1, Immunity (2011), doi:10.1016/j.immuni.2010.12.010

Raab, M., Wang, H., Lu, Y., Smith, X., Wu, Z., Strebhardt, K., Ladbury, J.E., and Rudd, C.E. (2010). T cell receptor "inside-out" pathway via signaling module SKAP1-RapL regulates T cell motility and interactions in lymph nodes. Immunity *32*, 541–556.

Reynisdottir, I., and Massague, J. (1997). The subcellular locations of p15 (Ink4b) and p27(Kip1) coordinate their inhibitory interactions with cdk4 and cdk2. Genes Dev. *11*, 492–503.

Rodier, G., Montagnoli, A., Di Marcotullio, L., Coulombe, P., Draetta, G.F., Pagano, M., and Meloche, S. (2001). p27 cytoplasmic localization is regulated by phosphorylation on Ser10 and is not a prerequisite for its proteolysis. EMBO J. *20*, 6672–6682.

Semmrich, M., Smith, A., Feterowski, C., Beer, S., Engelhardt, B., Busch, D.H., Bartsch, B., Laschinger, M., Hogg, N., Pfeffer, K., and Holzmann, B. (2005). Importance of integrin LFA-1 deactivation for the generation of immune responses. J. Exp. Med. *201*, 1987–1998.

Sherr, C.J., and Roberts, J.M. (1999). Cdk inhibitors: Positive and negative regulators of G1-phase progression. Genes Dev. *13*, 1501–1512.

Stork, P.J., and Dillon, T.J. (2005). Multiple roles of Rap1 in hematopoietic cells: Complementary versus antagonistic functions. Blood *106*, 2952–2961.

Tan, J.T., Dudl, E., LeRoy, E., Murray, R., Sprent, J., Weinberg, K.I., and Surh, C.D. (2001). IL-7 is critical for homeostatic proliferation and survival of naive T cells. Proc. Natl. Acad. Sci. USA *98*, 8732–8737.

Vos, M.D., Martinez, A., Ellis, C.A., Vallecorsa, T., and Clark, G.J. (2003). The pro-apoptotic Ras effector Nore1 may serve as a Ras-regulated tumor suppressor in the lung. J. Biol. Chem. *278*, 21938–21943.

ARTHRITIS & RHEUMATISM
Vol. 64, No. 1, January 2012, pp 254–263
DOI 10.1002/art.33320

Th2 and Regulatory Immune Reactions Contribute to IgG4 Production and the Initiation of Mikulicz Disease

Akihiko Tanaka,[1] Masafumi Moriyama,[1] Hitoshi Nakashima,[2] Katsuhisa Miyake,[2] Jun-Nosuke Hayashida,[1] Takashi Maehara,[1] Shouichi Shinozaki,[1] Yoshiaki Kubo,[1] and Seiji Nakamura[1]

Objective. **Mikulicz disease has been considered to be a subtype of Sjögren's syndrome (SS). However, recent studies have suggested that Mikulicz disease is an IgG4-related disease and is distinguishable from SS. In addition, it has been reported that both interleukin-4 (IL-4) and IL-10 induce IgG4 production and inhibit IgE. This study was undertaken to examine the expression of these cytokines in patients with Mikulicz disease and patients with SS.**

Methods. **Labial salivary gland (LSG) sections from 15 patients with Mikulicz disease and 18 patients with SS were examined for subsets of the infiltrating lymphocytes, expression patterns of messenger RNA (mRNA) for cytokines/chemokines, and relationships between the IgG4:IgG ratio and the expression of mRNA for IL-4 or IL-10.**

Results. **Immunohistochemical analysis showed lymphocyte infiltration of various subsets in the LSGs of SS patients, and the selective infiltration of IgG4-positive plasma cells and Treg cells in the LSGs of Mikulicz disease patients. The levels of mRNA for both Th1 and Th2 cytokines and chemokines in LSGs from patients with SS were significantly higher than in controls, while the expression of both Th2 and Treg cells was significantly higher in the patients with Mikulicz disease than in controls. Furthermore, the expression of IL-4 or IL-10 in the LSGs was correlated with the IgG4:IgG ratio.**

Conclusion. **These results suggest that the pathogenesis of Mikulicz disease is different from that of SS. Mikulicz disease is a unique inflammatory disorder characterized by Th2 and regulatory immune reactions that might play key roles in IgG4 production.**

Mikulicz disease has been considered to be a subtype of Sjögren's syndrome (SS), based on the histopathologic similarities between the two diseases (1). However, Mikulicz disease shows several differences in comparison with typical SS. In Mikulicz disease, enlargement of the lacrimal and salivary glands is persistent, salivary secretion is either normal or moderately dysfunctional, patients have a good response to corticosteroid treatment, and hypergammaglobulinemia and low frequencies of anti-SSA and anti-SSB antibodies are found on serologic analyses. Since Yamamoto et al (1–3) reported that serum IgG4 levels are elevated and IgG4-positive plasma cells infiltrate into the gland tissue in Mikulicz disease, these symptoms have also been recognized in autoimmune pancreatitis (4), primary sclerosing cholangitis (5), tubulointerstitial nephritis (6), interstitial pneumonia (7), Ridel's thyroiditis (8), and Küttner's tumor (9). These diseases are now called "IgG4-related diseases" (2,10). IgG4 is a Th2-dependent Ig and has low affinity for target antigen. Interleukin-4 (IL-4) directs naive human B cells to switch to IgG4 and IgE production (11).

CD4+ T helper cells including at least 5 subsets have been identified. Th0, Th1, Th2, Th17, and Treg cells are generally considered to maintain the balance

Supported in part by the Ministry of Education, Culture, Sports, Science, and Technology of Japan (grant 22791990) and the Ministry of Health, Labor, and Welfare of Japan (Health and Labor Sciences Research, Research on Intractable Diseases Program grant).

[1]Akihiko Tanaka, DDS, PhD, Masafumi Moriyama, DDS, PhD, Jun-Nosuke Hayashida, DDS, PhD, Takashi Maehara, DDS, Shouichi Shinozaki, DDS, PhD, Yoshiaki Kubo, DDS, Seiji Nakamura, DDS, PhD: Kyushu University, Fukuoka, Japan; [2]Hitoshi Nakashima, MD, PhD, Katsuhisa Miyake, MD, PhD: Fukuoka University, Fukuoka, Japan.

Drs. Tanaka and Moriyama contributed equally to this work.

Address correspondence to Seiji Nakamura, DDS, PhD, Section of Oral and Maxillofacial Oncology, Division of Maxillofacial Diagnostic and Surgical Sciences, Faculty of Dental Science, Kyushu University, 3-1-1 Maidashi, Higashi-ku, Fukuoka 812-8582, Japan. E-mail: seiji@dent.kyushu-u.ac.jp.

Submitted for publication December 6, 2010; accepted in revised form August 25, 2011.

and homeostasis of the immune system and possibly to induce various diseases by their impaired regulation. The difference in the functions of Th1 and Th2 cells has been characterized by the patterns of cytokines secreted by these Th cells. Th1 cells induced by IL-12 are mainly responsible for cell-mediated immunity, while Th2 cells induced by IL-4 are responsible for humoral immunity. These Th subsets are then mutually controlled by the cytokine that each produces. Several studies have indicated that many autoimmune diseases or allergic diseases are caused by the collapse of the Th1/Th2 balance. Th0 cells are produced by both Th1 and Th2 cytokines and are considered to be precursors of Th1 and Th2 cells. Treg cells are essential for the maintenance of immunologic self-tolerance and immune homeostasis. Recently, a subset of IL-17–producing T cells (Th17 cells) distinct from Th1 and Th2 cells was described and was shown to play a crucial role in the induction of autoimmunity and allergic inflammation (12). Furthermore, it has been demonstrated that chemokines are intimately involved in the Th1/Th2 balance and immune responses in various diseases, such as rheumatoid arthritis (13), systemic lupus erythematosus (13,14), SS (13,15), systemic sclerosis (13,16), idiopathic inflammatory myopathy (13), and atopic dermatitis (17).

The relationship of Th1/Th2 imbalance to the pathogenesis of SS has been investigated widely, and a polarized Th1 balance has been associated with the immunopathology of the disease (18–20). Numerous interferon-γ (IFNγ)–positive CD4+ T cells are detected in the salivary glands of SS patients, and an intracellular cytokine assay demonstrated subsequent promotion of Th1 cells in SS (21). We have previously shown that SS was initiated and/or maintained by Th1 cytokines and subsequently progressed in association with Th2 cytokines (22). Ogawa et al (15) reported that Th1 chemokines, such as IFNγ-inducible 10-kd protein (IP-10) and monokine induced by IFNγ, are involved in the accumulation of T cell infiltrates in the salivary glands of patients with SS. These findings suggest that Th1 cells play a central role in the pathogenesis of SS.

In contrast, patients with Mikulicz disease frequently have a history of bronchial asthma and allergic rhinitis and show severe eosinophilia and elevated serum IgE levels. We previously reported that peripheral CD4+ T cells from patients with Mikulicz disease revealed deviation of the Th1/Th2 balance to Th2 and elevated the expression of Th2-type cytokines (23,24). Moreover, recent studies have indicated that peripheral blood CD4+ T cells in patients with IgG4-related lacrimal gland enlargement showed a Th2 bias and elevated serum IgE levels (24). Therefore, it is suggested that Mikulicz disease has a Th2-predominant phenotype. The findings of a previous study showing that autoimmune pancreatocholangitis, which is an IgG4-related disease, could also be characterized by the overproduction of Th2 and regulatory cytokines (25) deserve our attention.

To date, pathogenetic differences between immune responses in SS and Mikulicz disease are not well understood. In this study, we identified the expression patterns of cytokines, chemokines, and chemokine receptors in the salivary glands of these diseases to clarify the involvement of characteristic immune responses in the development of Mikulicz disease.

PATIENTS AND METHODS

Patients. Fifteen patients with Mikulicz disease (12 women and 3 men with a mean ± SD age of 56.3 ± 13.0 years) and 18 patients with SS (16 women and 2 men with a mean ± SD age of 54.6 ± 12.8 years) who were referred to the Department of Oral and Maxillofacial Surgery at Kyushu University Hospital were included in the study. Mikulicz disease was diagnosed according to the following criteria (3): persistent symmetrical swelling (lasting longer than 3 months) of >2 lacrimal and major salivary glands, elevated serum levels of IgG4 (>135 mg/dl), and infiltration of IgG4-positive plasma cells in the tissue (ratio of IgG4-positive cells:IgG-positive cells >40%) on immunostaining. SS was diagnosed according to the criteria of both the Research Committee on SS of the Ministry of Health and Welfare of the Japanese Government (1999) (26) and the American–European Consensus Group criteria for SS (27).

All patients exhibited objective evidence of salivary gland involvement based on the presence of subjective xerostomia and a decreased salivary flow rate, abnormal findings on parotid sialography, and focal lymphocytic infiltrates in the labial salivary glands (LSGs) and submandibular glands. All patients with SS had primary SS with strong lymphocytic infiltration in the LSGs, had no other autoimmune diseases, and had never been treated with corticosteroids or any other immunosuppressants. LSG biopsies were performed as described by Greenspan et al (28). As controls, LSGs biopsy specimens were obtained from 18 patients with mucoceles who had no clinical or laboratory evidence of systemic autoimmune disease. These control LSGs were all histologically normal. Written informed consent was obtained from all patients and healthy controls.

Histologic analysis of LSGs. Formalin-fixed and paraffin-embedded sections (4 μm) of LSG specimens were prepared and stained with hematoxylin and eosin for conventional histologic examinations. The degree of lymphocytic infiltration in the specimens was judged by focus scoring (28,29). One standardized score is the number of focal inflammatory cell aggregates containing 50 or more mononuclear cells in each 4-mm^2 area of salivary gland tissue (30). All of the patients with Mikulicz disease and patients with SS

in this study had strong lymphocytic infiltration (focus scores of 10–12).

Immunohistochemical analysis of LSGs. For the immunohistochemical analysis of lymphocyte subsets, 4-μm formalin-fixed and paraffin-embedded sections were prepared and stained by a conventional avidin–biotin complex technique as previously described (31). The mouse monoclonal antibodies used to analyze lymphocyte subsets were anti-CD4 (clone B12; MBL), anti-CD20 (clones L26 and M0755; Dako), and anti-FoxP3 (clone mAbcam 22510; Abcam). The mouse monoclonal antibody and rabbit polyclonal antibody used to analyze IgG4-positive and IgG-positive plasma cells were anti-IgG (A0423; Dako) and anti-IgG4 (The Binding Site). HDP-1 (antidinitrophenyl [anti-DNP] IgG1) was used as a control mouse monoclonal antibody. The polyclonal antibodies used to analyze the cytokines were anti–IL-4 (clone ab9622), anti–IL-10 (clone ab34843), anti–IFNγ (clone ab9657) (all from Abcam), and anti–IL-17 (clone sc-7927; Santa Cruz Biotechnology). SS1 (anti–sheep erythrocyte IgG2a), NS8.1 (anti–sheep erythrocyte IgG2b), and NS4.1 (anti–sheep erythrocyte IgM), were used as control rabbit polyclonal antibodies. The mouse monoclonal antibodies used to analyze the chemokines and chemokine receptors were anti–IP-10 (clone ab73837; Abcam), anti-CXCR3 (clone ab64714; Abcam), anti–thymus and activation–regulated chemokine (anti-TARC) (54015; R&D Systems), anti–macrophage-derived chemokine (anti-MDC) (57203; R&D Systems), and anti-CCR4 (MAB1567; R&D Systems). HDP-1 (anti-DNP IgG1) was used as a control mouse monoclonal antibody. The sections were sequentially incubated with primary antibodies, biotinylated anti-mouse IgG secondary antibodies (Vector Laboratories), avidin–biotin–horseradish peroxidase complex (Vector Laboratories), and 3,3′-diaminobenzidine (Vector Laboratories). Mayer's hematoxylin was used for counterstaining. Photomicrographs were obtained using a light microscope equipped with a digital camera (CoolSNAP; Photometrics). Stained IgG4-positive cells and IgG-positive cells were counted in 1-mm^2 sections from 5 different areas, and the ratio of IgG4-positive cells to IgG-positive cells was calculated.

RNA extraction and complementary DNA (cDNA) synthesis. Total RNA was prepared from the LSG specimens by the acid guanidinium–phenol–chloroform method as previously described (32–34). Three micrograms of the total RNA preparation was then used for the synthesis of cDNA. Briefly, RNA was incubated for 1 hour at 42°C with 20 units of RNasin ribonuclease inhibitor (Promega), 0.5 μg of oligo(dT)$_{12\text{-}18}$ (Pharmacia), 0.5 m*M* of each dNTP (Pharmacia), 10 m*M* of dithiothreitol, and 100 units of RNase H reverse transcriptase (Life Technologies).

Quantitative estimation of messenger RNA (mRNA) by real-time polymerase chain reaction (PCR). Quantitative cDNA amplification was performed according to the recommendations of the manufacturer and as previously described (32–34). The cDNAs for the cytokines, chemokines, and chemokine receptors were analyzed by real-time PCR using LightCycler FastStart DNA Master SYBR Green 1 (Roche Diagnostics) in a LightCycler real-time PCR instrument (version 3.5; Roche Diagnostics). The cytokines, chemokines, and chemokine receptors examined were IL-2, IFNγ, IL-12, IP-10, CXCR3, IL-4, IL-5, TARC, MDC, CCR4, IL-10, transforming growth factor β (TGFβ), FoxP3, IL-17, and IL-6. The markers of lymphocytes examined were IgG and IgG4.

The primer sequences used were as follows: for β-actin (260 bp), forward 5′-GCAAAGACCTG-TACGCCAAC-3′, reverse 5′-CTAGAAGCATTTGCGGTGGA-3′; for CD3δ (184 bp), forward 5′-GATGTCATTGCCACTCTGC-3′, reverse 5′-ACTTGTTCCGAGCCCAGTT-3′; for IL-2 (416 bp), forward 5′-ACTCACCAGGATGCTCACAT-3′, reverse 5′-AGGTAATCCATCTG-TTCAGA-3′; for IFNγ (355 bp), forward 5′-AGTTATATCTTGGCTTTTCA-3′, reverse 5′-ACCGAATAATTAGTCAGCTT-3′; for IL-4 (203 bp), forward 5′-CTGCCTCCAAGAACACAACT-3′, reverse 5′-CACAGGACAGGAATTCAAGC-3′; for IL-5 (104 bp), forward 5′-ATGAGGATGCTTCTGCATTTG-3′, reverse 5′-TCAACTTTCTATTATCCACTCG-3′; for IL-6 (115 bp),

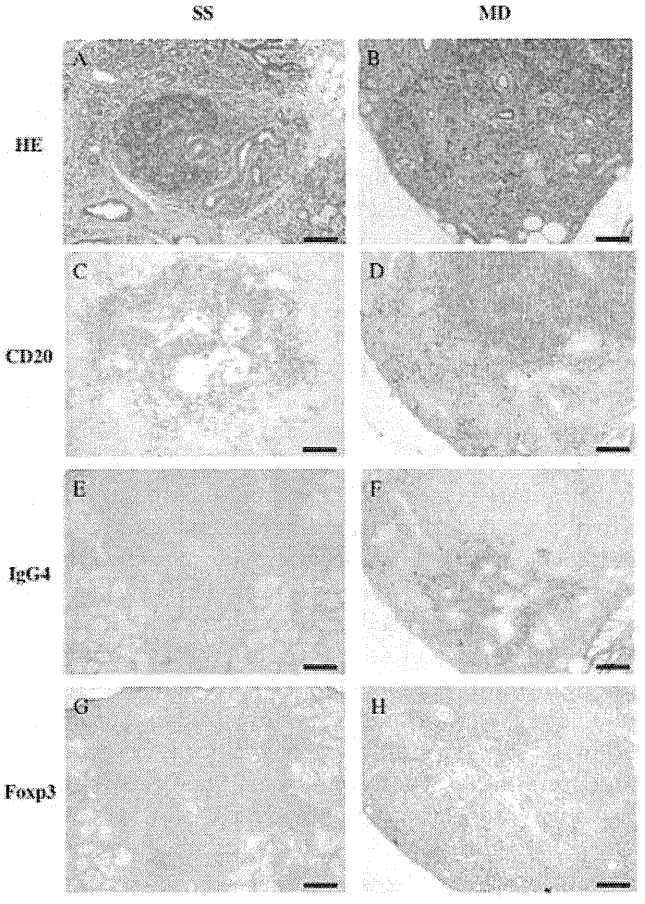

Figure 1. Selective infiltration of IgG4-positive plasma cells and FoxP3-positive Treg cells in the labial salivary glands (LSGs) of patients with Mikulicz disease (MD). Sections from the LSGs of a representative patient with Sjögren's syndrome (SS) and a representative patient with Mikulicz disease were immunostained with hematoxylin and eosin (H&E) (**A** and **B**) and anti-CD20 (**C** and **D**), anti-IgG4 (**E** and **F**), and anti-FoxP3 (**G** and **H**) monoclonal antibodies. Counterstaining with Mayer's hematoxylin was subsequently performed. Bars = 100 mm; original magnification × 100.

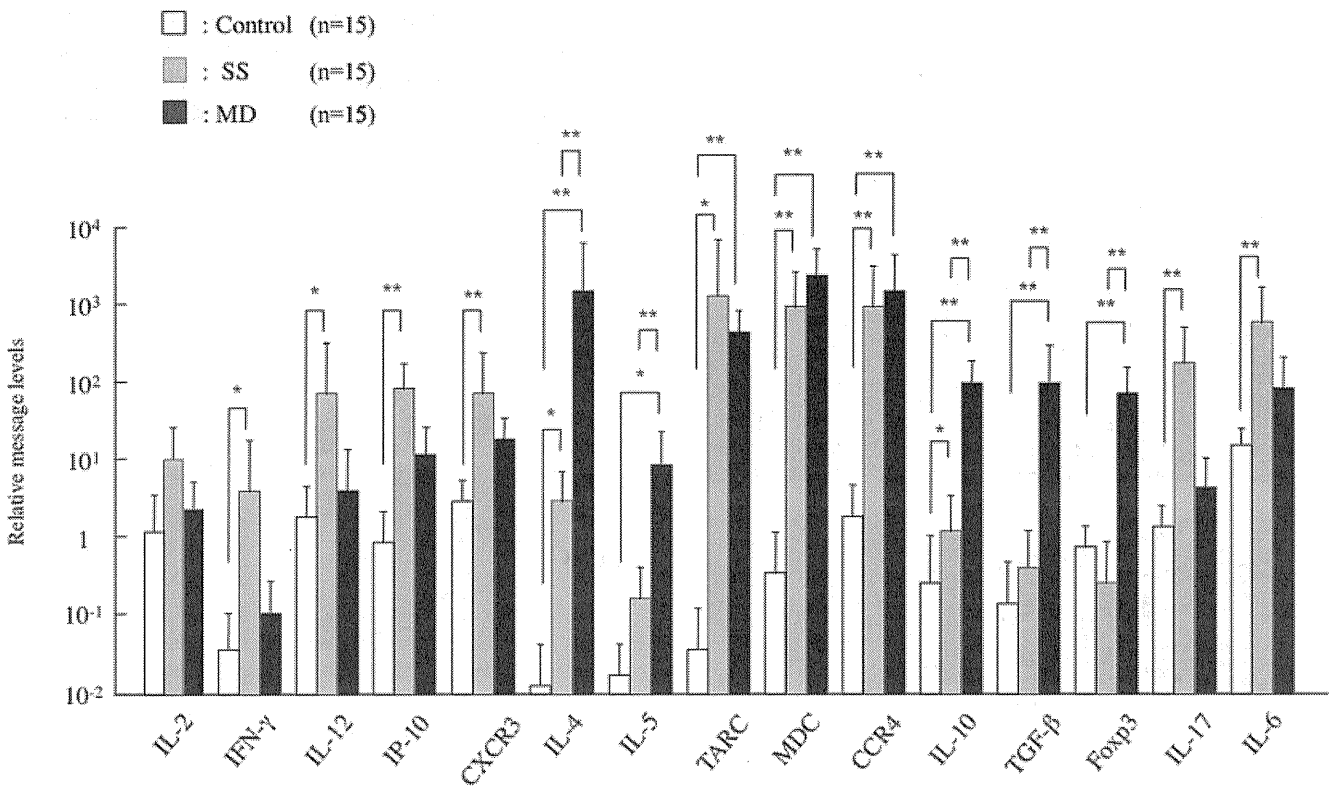

Figure 2. Expression patterns of mRNA for cytokines, chemokines, and chemokine receptors in LSGs from controls, patients with SS, and patients with Mikulicz disease. Levels of interferon-γ (IFNγ), interleukin-2 (IL-2), IL-12, IFNγ-inducible 10-kd protein (IP-10), and CXCR3 (Th1 type); IL-4, IL-5, thymus and activation–regulated chemokine (TARC), macrophage-derived chemokine (MDC), and CCR4 (Th2 type); IL-10, transforming growth factor β (TGFβ), and FoxP3 (Treg cell type); and IL-6 and IL-17 (Th17 type) were quantitatively estimated as described in Patients and Methods. Levels of mRNA in LSGs from SS patients and patients with Mikulicz disease were compared with those in control LSGs. Bars show the mean ± SD. * = $P < 0.05$; ** = $P < 0.01$ by Mann-Whitney U test. See Figure 1 for other definitions.

forward 5′-GGCACTGGCAGAAAACAA-3′, reverse 5′-CTCCAAAAGACCAGTGATGA-3′; for IL-10 (351 bp), forward 5′-ATGCCCCAAGCTGAGAACCAA-3′, reverse 5′-TCTCAAGGGGCTGGGTCAGCTA-3′; for IL-12 (187 bp), forward 5′-CCTGACCCACCCAAGAACTT-3′, reverse 5′-GTGGCTGAGGTCTTGTCCGT-3′; for IL-17 (186 bp), forward 5′-GCAGGAATCACAATCCCAC-3′, reverse 5′-TCTCTCAGGGTCCTCATTGC-3′; for FoxP3 (207 bp), forward 5′-CCCCTTGCCCCACTTACA-3′, reverse 5′-GCCACGTTGATCCCAGGT-3′; for TGFβ (142 bp), forward 5′-GCCCCTACATTTGGAGCCTG-3′, reverse 5′-TTGCGGCCCACGTAGTACAC-3′; for IgG (129 bp), forward 5′-CAAGTGCAAGGTCTCCAACA-3′, reverse 5′-TGGTTCTTGGTCAGCTCATC-3′; for IgG4 (132 bp), forward 5′-ACTCTACTCCCTCAGCAGCG-3′, reverse 5′-GGGGGACCATATTTGGAC-3′; for IP-10 (288 bp), forward 5′-CCTTAAAACCAGAGGGGAGC-3′, reverse 5′-AGCAGGGTCAGAACATCCAC-3′; for CXCR3 (184 bp), forward 5′-CTGGTGGTGCTGGTGGACAT-3′, reverse 5′-AGAGCAGCATCCACATCCG-3′; for MDC (253 bp), forward 5′-CGCGTGGTGAAACACTTCTA-3′, reverse 5′-GAATGCAGAGAGTTGGCACA-3′; for TARC (140 bp), forward 5′-TAGAAAGCTGAAGACGTGGT-3′, reverse 5′-GGCTTTGCAGGTATTTAACT-3′; for CCR4 (214 bp), forward 5′-GTGCTCTGCCAATACTGTGG-3′, reverse 5′-CTTCCTCCTGACACTGGCTC-3′; and for CD3α (184 bp), forward 5′-GATGTCATTGCCACTCTGC-3′, reverse 5′-ACTTGTTCCGAGCCCAGTT-3′.

In order to provide a meaningful comparison between different individuals or samples, we calculated the relative amounts of the PCR products of these molecules to the amounts of the PCR products of CD3δ (for the standardization of T cell mRNA) or the PCR products of β-actin (for the standardization of total cellular mRNA) in each sample, as previously described (22,23,35,36). The CD3δ PCR product levels were used for T cell–specific molecules, such as IL-2, IL-5, IL-12, and IFNγ, while the β-actin PCR product levels were used for T cell–nonspecific molecules, such as IL-4, IL-6, IL-10, IL-17, and chemokines, which were produced by a variety of cell types.

Statistical analysis. The statistical significance of the differences between the groups was determined by the Mann-Whitney U test and Spearman's rank correlation. All statistical analyses in this study were performed using JMP software, version 8 (SAS Institute). *P* values less than 0.05 were considered significant.

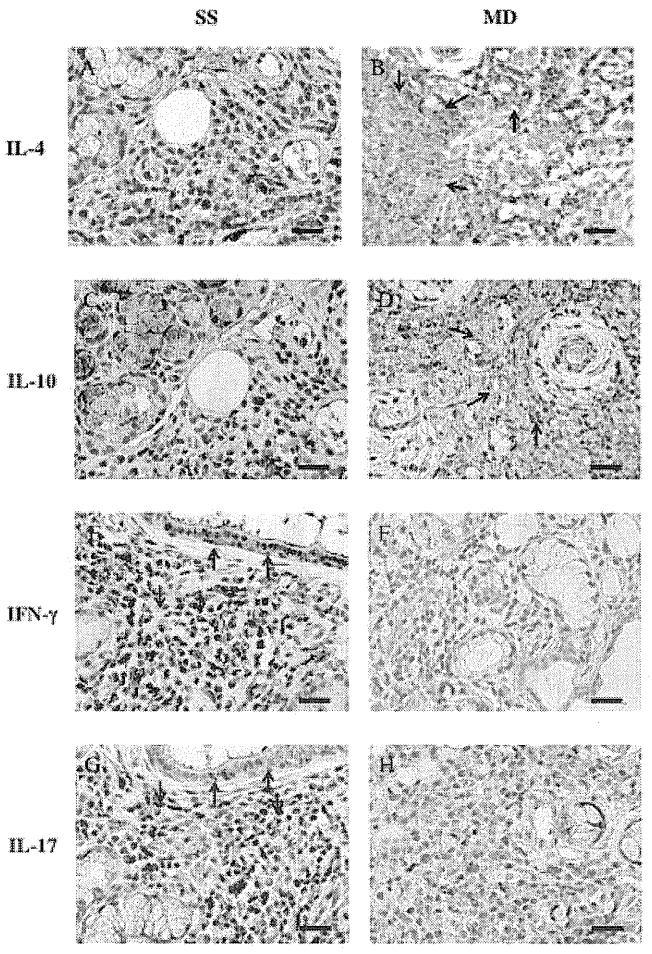

Figure 3. Expression of interleukin-10 (IL-10), IL-4, interferon-γ (IFNγ), and IL-17 in LSG specimens from patients with SS and patients with Mikulicz disease. IL-10 and IL-4 were prominently expressed around the germinal centers in LSG specimens from patients with Mikulicz disease. Sections from LSGs of a representative patient with SS and a representative patient with Mikulicz disease were immunostained with anti–IL-10 (**A** and **B**), anti–IL-4 (**C** and **D**), anti-IFNγ (**E** and **F**), and anti–IL-17 (**G** and **H**) polyclonal antibodies. Counterstaining with Mayer's hematoxylin was subsequently performed. **Arrows** indicate key features of infiltrating cells. Bars = 50 mm; original magnification × 400. See Figure 1 for other definitions.

RESULTS

Results of histologic analysis of lymphocyte subsets in the LSGs. Representative sections showing histologic findings and lymphocyte subsets in LSG specimens from patients with Mikulicz disease and patients with SS are shown in Figure 1. Specimens from patients with SS showed lymphocytic infiltration of various subsets with atrophy or severe destruction of the acini, while specimens from patients with Mikulicz disease showed selective infiltration of IgG4-positive plasma cells and FoxP3-positive Treg cells around the acinar and ductal cells with a lot of lymphoid follicles and mild destruction of the acini.

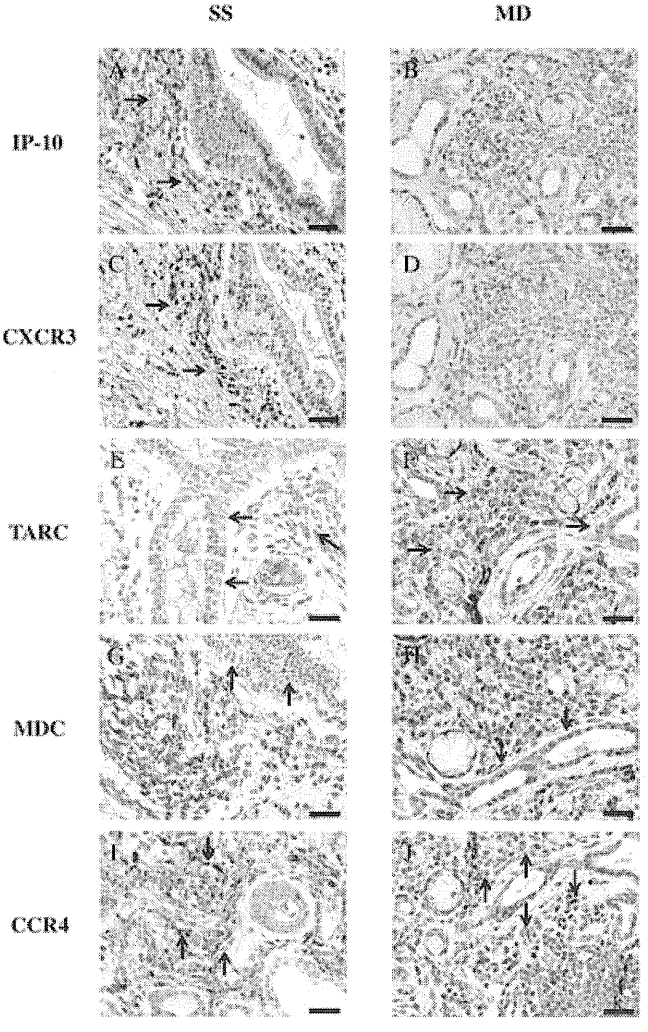

Figure 4. Expression of interferon-γ–inducible 10-kd protein (IP-10), CXCR3, thymus and activation–regulated chemokine (TARC), macrophage-derived chemokine (MDC), and CCR4 in LSG specimens from patients with SS and patients with Mikulicz disease. TARC and MDC were strongly expressed around the germinal centers in LSG specimens from patients with Mikulicz disease. Sections from LSGs of a representative patient with SS and a representative patient with Mikulicz disease were immunostained with anti–IP-10 (**A** and **B**), anti-CXCR3 (**C** and **D**), anti-TARC (**E** and **F**), anti-MDC (**G** and **H**), and anti-CCR4 (**I** and **J**) monoclonal antibodies. Counterstaining with Mayer's hematoxylin was subsequently performed. **Arrows** indicate key features of infiltrating cells. Bars = 50 mm; original magnification × 400. See Figure 1 for other definitions.

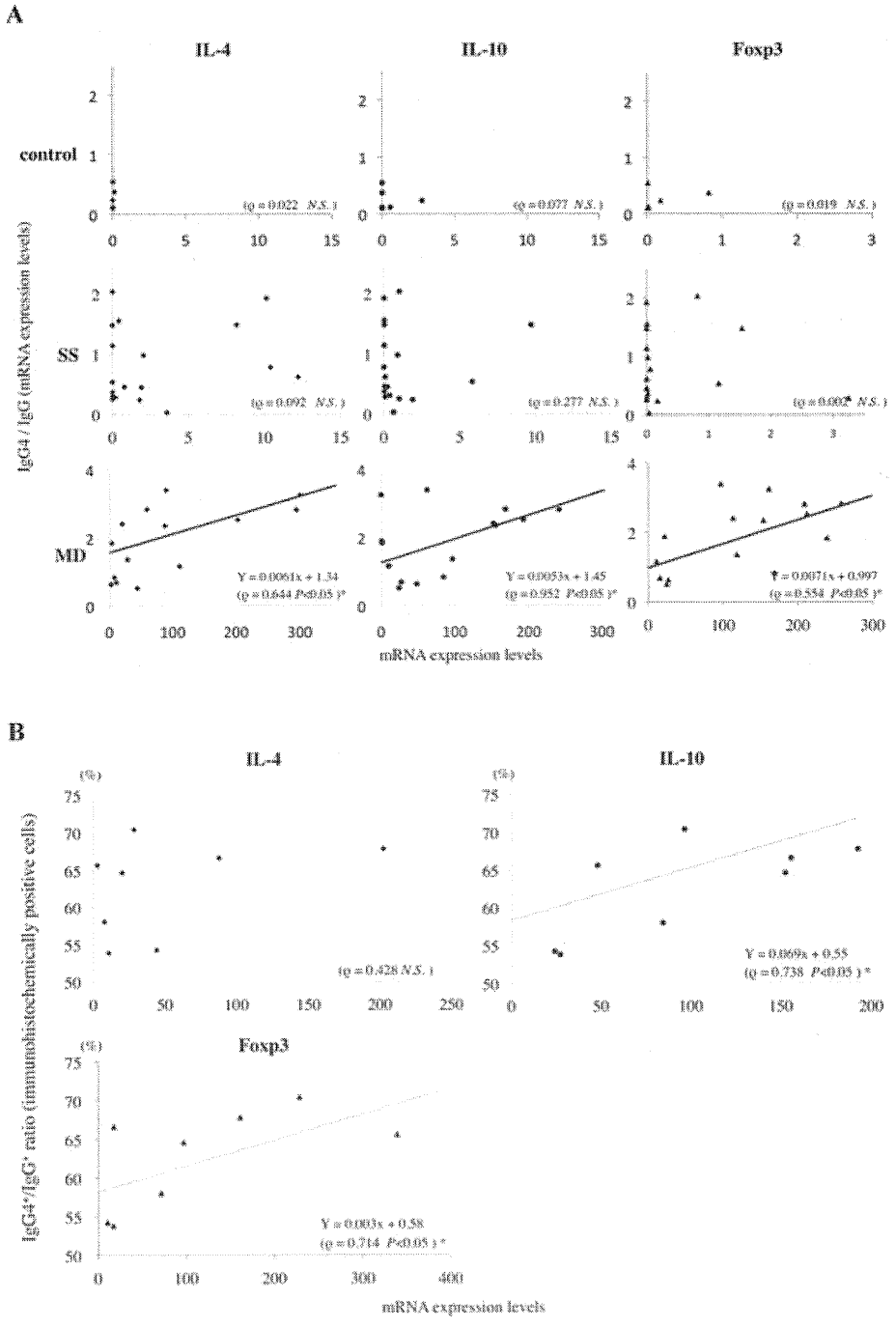

Figure 5. Correlation of the production of IgG4 with the production of interleukin-4 (IL-4), IL-10, and FoxP3 in LSGs from patients with Mikulicz disease. **A,** Correlations between the ratio of IgG4 mRNA to IgG mRNA and the expression of mRNA for IL-4, IL-10, and FoxP3 in LSGs from patients with SS, patients with Mikulicz disease, and healthy controls. Real-time polymerase chain reaction products for IL-4, IL-10, FoxP3, IgG, and IgG4 were quantitatively estimated as described in Patients and Methods. The ratio was calculated as IgG4-positive cells (%) = IgG4-positive cells/IgG-positive cells × 100. The counts were obtained in 1-mm^2 sections from 5 different areas. **B,** Correlations between the frequencies of IgG4-positive cells and the expression of mRNA for IL-4, IL-10, and FoxP3 in LSGs from patients with Mikulicz disease. $* = P < 0.05$ by Spearman's rank correlation. NS = not significant (see Figure 1 for other definitions).

Expression of mRNA for cytokines, chemokines, and chemokine receptors in the LSGs. In order to compare the expression of mRNA for cytokines, chemokines, and chemokine receptors in LSGs from patients with Mikulicz disease and LSGs from patients with SS, the relative expression compared to CD3δ was estimated and compared for cytokines and chemokine receptors primarily expressed by T cells, and the relative expression compared to β-actin was estimated for cytokines and chemokines produced by a variety of cell types.

The expression of mRNA for IFNγ, IL-12, IP-10, CXCR3, IL-4, TARC, MDC, CCR4, IL-10, IL-17, and IL-6 in LSGs from SS patients were higher than those in control LSGs (Figure 2). The expression of mRNA for IL-4, IL-5, TARC, MDC, CCR4, IL-10, TGFβ, and FoxP3 in LSGs from patients with Mikulicz disease were higher than those in control LSGs (Figure 2). In addition, the levels of expression of mRNA for IL-4, IL-5, IL-10, TGFβ, and FoxP3 in LSGs from patients with Mikulicz disease were higher than in LSGs from patients with SS (Figure 2).

Protein levels of cytokines, chemokines, and chemokine receptors in the LSGs. The specimens were immunohistochemically examined to evaluate the distributions of these proteins in LSGs from patients with SS and patients with Mikulicz disease. The Th1-type cytokine IFNγ and Th17-type cytokine IL-17 were strongly expressed and detected in and around the ductal epithelial cells in LSGs from SS patients only (Figures 3E and G). Although IL-10 and IL-4 were detected in LSGs from both patients with Mikulicz disease and patients with SS, they were prominently expressed around germinal centers in LSGs from Mikulicz disease patients but not in LSGs from SS patients (Figures 3B and D). In LSGs from patients with SS, IP-10 and CXCR3 were detected in a higher number of infiltrating lymphocytes than in LSGs from patients with Mikulicz disease (Figures 4A and C). In LSGs from patients with Mikulicz disease, TARC and MDC were strongly expressed, especially around germinal centers (Figures 4F and H). In LSGs from both patients with SS and patients with Mikulicz disease, CCR4 was detected in high numbers of infiltrating lymphocytes (Figures 4I and J).

Relationship between IgG4 production and cytokine expression in the LSGs. The relationships between IgG4 production and the expression of mRNA for IL-4, IL-10, and FoxP3 in the LSGs were examined. These molecules were all positively correlated with the ratio of IgG4 mRNA to IgG mRNA in LSGs from patients with Mikulicz disease, but no relationships were confirmed in those from SS patients (Figure 5A). Furthermore, IL-10 mRNA and FoxP3 mRNA in LSGs from patients with Mikulicz disease were correlated with the ratio of IgG4 to IgG in immunohistochemically positive cells (Figure 5B).

DISCUSSION

Mikulicz disease presents with bilateral and persistent swelling of the lacrimal and salivary glands, and it has been considered to be part of primary SS or a subtype of primary SS since the findings by Morgan and Castleman were published in 1953 (37). However, Yamamoto et al (38,39) reported differences in the clinical and histopathologic findings between Mikulicz disease and SS. Serologically, Mikulicz disease patients show hypergammaglobulinemia, hypocomplementemia, and high levels of serum IgG4, but are negative for anti-SSA and anti-SSB antibodies. Immunohistologic analysis of samples from patients with Mikulicz disease revealed the selective infiltration of IgG4-positive plasma cells, which was not observed near acinar and ductal cells. In contrast, similar specimens from SS patients showed no IgG4-positive plasma cells (38,39). In this study, samples from patients with Mikulicz disease showed selective infiltration of IgG4-positive plasma cells and FoxP3-positive cells around acinar and ductal cells with mild destruction of the acini, while samples from patients with SS showed no infiltration of IgG4-positive plasma cells and FoxP3-positive cells, and had atrophy or severe destruction of acini (Figure 1).

In order to examine the differences in infiltrating lymphocytes between LSGs from patients with SS and LSGs from patients with Mikulicz disease, we analyzed the levels of cytokines, chemokines, and chemokine receptors. The levels of Th1-, Th2-, and Th17-type molecules in LSGs from SS patients were significantly higher than those in LSGs from controls. The levels of Th2 and Treg-type molecules in LSGs from patients with Mikulicz disease were significantly higher than those in LSGs from controls. Furthermore, immunohistochemical staining indicated that IFNγ and IL-17 were strongly detected in and around ductal epithelial cells in LSGs from SS patients only, while IL-4 and IL-10 were detected in LSGs from both patients with SS and patients with Mikulicz disease. In particular, these cytokines were prominently expressed around germinal centers in specimens from patients with Mikulicz disease but not in specimens from patients with SS.

It is generally accepted that CD4+ Th cells play a crucial role in the pathogenesis of SS. Several studies of autoimmune diseases have demonstrated pathoge-

netic roles for Th1 cells and the possible protective role for Th2 cells (40,41). Our previous studies of SS suggested that the mutual stimulation of Th1 cells and their target organs via the production of various cytokines plays a key role in the induction and maintenance of SS and results in the eventual destruction of the target organ (22,42,43). Subsequently, additional Th2 cells then stimulate B cells to differentiate, proliferate, and produce immunoglobulins and, thus, play a role in the lymphoaggressiveness of SS. Regarding the possible roles of Th2 cells in the induction of B cell abnormalities, these cells might have an important association with the progression of SS. In contract, Zen et al (25) reported that autoimmune pancreatocholangitis, an IgG4-related disease, is characterized by immune reactions that are predominantly mediated by Th2 cells and Treg cells.

The results of the present study concerning the levels of cytokines, chemokines, and chemokine receptors in the LSGs are consistent with the model of SS and Mikulicz disease as distinct diseases. Immunohistochemical staining indicated that MDC and TARC were detectable in and around the ductal epithelial cells and germinal centers, while CCR4 was expressed on the infiltrating lymphocytes in the LSGs in both SS patients and patients with Mikulicz disease. The interactions of CCR4 with MDC and TARC are suggested to play a critical role in the accumulation of Th2 cells and, consequently, the progression of SS and Mikulicz disease. TARC and MDC are natural ligands for CCR4 on Th2 cells (44,45). In contrast, IP-10 was detected in and around the ductal epithelial cells, while CXCR3 was expressed on the infiltrating lymphocytes in the LSGs in SS patients only. IP-10 is a natural ligand for CXCR3 on Th1 cells (15).

It is well known that allergic immune responses are the development of allergen-specific Th2-type cytokines IL-4 and IL-13, which are responsible for IgG4 and IgE induced by B cells (46). In our previous studies, we demonstrated that Th2 immune reactions contributed to Mikulicz disease and IgG4-related tubulointerstitial nephritis (23,24,35). The expression profile of cytokines demonstrated in this study suggested that Mikulicz disease was characterized by an intense expression of Th2 and regulatory cytokines (Figure 2). In addition, recent studies have shown that class switching of IgG4 is caused by costimulation with IL-4 and IL-10, and that IL-10 decreased IL-4–induced IgE switching but elevated IL-4-induced IgG4 production (47).

Treg cells exert their effects through the modulation of both T and B cell responses, and two subsets of

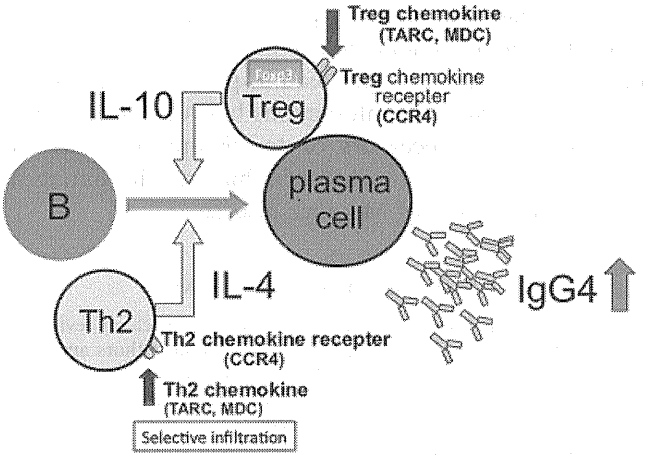

Figure 6. Schematic model of the mechanisms underlying IgG4 production. TARC = thymus and activation–regulated chemokine; MDC = macrophage-derived chemokine; IL-10 = interleukin-10.

Treg cells, CD4+CD25+FoxP3+ Treg cells (48) and IL-10–producing Tr1 cells (49), are crucial in regulating effector T cell function. CD4+CD25+FoxP3+ Treg cells are known to affect the pathogenesis of cases of autoimmune hepatitis and primary biliary cirrhosis (50). Miyoshi et al (51) showed a positive correlation between the number of mature Treg cells ($CD4+CD25^{high}$ Treg cells) and IgG4. These results indicated that increased numbers of $CD4+CD25^{high}$ Treg cells may influence IgG4 production in autoimmune pancreatocholangitis, whereas decreased numbers of naive Treg cells (CD4+CD25+CD45RA+) may be involved in the pathogenesis of the disease (51). Therefore, we examined the relationships between IgG4 and IL-4, IL-10, and FoxP3.

We found that IL-4, IL-10, and FoxP3 were positively correlated with the ratio of IgG4 mRNA to IgG mRNA in samples from patients with Mikulicz disease analyzed by real-time PCR and comparison with the IgG4 to IgG ratio of immunohistochemically positive cells. In particular, IL-10 and FoxP3 levels were strongly correlated with IgG4 production. These results suggested that Th2 and Treg cells might be involved in the pathogenesis of Mikulicz disease. The findings of the present study provided additional support for the model of Mikulicz disease as distinct from SS (Figure 6). However, accumulation of case reports and further examinations are required to elucidate the pathogenesis of the disease.

In this study, we clarified the pathogenesis of Mikulicz disease and found that it is a unique IgG4-related disease, characterized by Th2 and regulatory

immune reactions, which apparently differs from SS. A more thorough understanding of the complex mechanisms of the disease might lead to pharmacologic strategies to interrupt the interactions between chemokines and chemokine receptors or to disrupt the cytokine network as a further means of inhibiting the initiation and/or progression of Mikulicz disease.

AUTHOR CONTRIBUTIONS

All authors were involved in drafting the article or revising it critically for important intellectual content, and all authors approved the final version to be published. Dr. Nakamura had full access to all of the data in the study and takes responsibility for the integrity of the data and the accuracy of the data analysis.

Study conception and design. Tanaka, Moriyama, Nakashima, Miyake, Nakamura.

Acquisition of data. Tanaka, Moriyama, Hayashida, Maehara, Shinozaki, Kubo.

Analysis and interpretation of data. Tanaka, Moriyama, Nakashima.

REFERENCES

1. Yamamoto M, Takahashi H, Sugai S, Imai K. Clinical and pathological characteristics of Mikulicz's disease (IgG4-related plasmacytic exocrinopathy). Autoimmun Rev 2005;4:195–200.
2. Yamamoto M, Takahashi H, Naishiro Y, Isshiki H, Ohara M, Suzuki C, et al. Mikulicz's disease and systemic IgG4-related plasmacytic syndrome (SIPS). Nihon Rinsho Meneki Gakkai Kaishi 2008;31:1–8.
3. Yamamoto M, Takahashi H, Ohara M, Suzuki C, Naishiro Y, Yamamoto H, et al. A new conceptualization for Mikulicz's disease as an IgG4-related plasmacytic disease. Mod Rheumatol 2006;16:335–40.
4. Hamano H, Kawa S, Horiuchi A, Unno H, Furuya N, Akamatsu T, et al. High serum IgG4 concentrations in patients with sclerosing pancreatitis. N Engl J Med 2001;344:732–8.
5. Zen Y, Harada K, Sasaki M, Sato Y, Tsuneyama K, Haratake J, et al. IgG4-related sclerosing cholangitis with and without hepatic inflammatory pseudotumor, and sclerosing pancreatitis-associated sclerosing cholangitis: do they belong to a spectrum of sclerosing pancreatitis? Am J Surg Pathol 2004;28:1193–203.
6. Takeda S, Haratake J, Kasai T, Takaeda C, Takazakura E. IgG4-associated idiopathic tubulointerstitial nephritis complicating autoimmune pancreatitis. Nephrol Dial Transplant 2004;19:474–6.
7. Zen Y, Kitagawa S, Minato H, Kurumaya H, Katayanagi K, Masuda S, et al. IgG4-positive plasma cells in inflammatory pseudotumor (plasma cell granuloma) of the lung. Hum Pathol 2005;36:710–7.
8. Hamed G, Tsushima K, Yasuo M, Kubo K, Yamazaki S, Kawa S, et al. Inflammatory lesions of the lung, submandibular gland, bile duct and prostate in a patient with IgG4-associated multifocal systemic fibrosclerosis. Respirology 2007;12:455–7.
9. Kitagawa S, Zen Y, Harada K, Sasaki M, Sato Y, Minato H, et al. Abundant IgG4-positive plasma cell infiltration characterizes chronic sclerosing sialadenitis (Kuttner's tumor). Am J Surg Pathol 2005;29:783–91.
10. Masaki Y, Umehara H. IgG4-related disease: the diagnostic confusion and how to avoid it. Nihon Rinsho Meneki Gakkai Kaishi 2009;32:478–83. In Japanese.
11. Punnonen J, Aversa G, Cocks BG, McKenzie AN, Menon S, Zurawski G, et al. Interleukin 13 induces interleukin 4-independent IgG4 and IgE synthesis and CD23 expression by human B cells. Proc Natl Acad Sci U S A 1993;90:3730–4.
12. Infante-Duarte C, Horton HF, Byrne MC, Kamradt T. Microbial lipopeptides induce the production of IL-17 in Th cells. J Immunol 2000;165:6107–15.
13. Lee EY, Lee ZH, Song YW. CXCL10 and autoimmune diseases. Autoimmun Rev 2009;8:379–83.
14. Fragoso-Loyo H, Richaud-Patin Y, Orozco-Narvaez A, Davila-Maldonado L, Atisha-Fregoso Y, Llorente L, et al. Interleukin-6 and chemokines in the neuropsychiatric manifestations of systemic lupus erythematosus. Arthritis Rheum 2007;56:1242–50.
15. Ogawa N, Ping L, Zhenjun L, Takada Y, Sugai S. Involvement of the interferon-γ–induced T cell–attracting chemokines, interferon-γ–inducible 10-kd protein (CXCL10) and monokine induced by interferon-γ (CXCL9), in the salivary gland lesions of patients with Sjögren's syndrome. Arthritis Rheum 2002;46:2730–41.
16. Antonelli A, Ferri C, Fallahi P, Ferrari SM, Giuggioli D, Colaci M, et al. CXCL10 (α) and CCL2 (β) chemokines in systemic sclerosis—a longitudinal study. Rheumatology (Oxford) 2008;47:45–9.
17. Miyahara H, Okazaki N, Nagakura T, Korematsu S, Izumi T. Elevated umbilical cord serum TARC/CCL17 levels predict the development of atopic dermatitis in infancy. Clin Exp Allergy 2011;41:186–91.
18. Fox RI, Kang HI, Ando D, Abrams J, Pisa E. Cytokine mRNA expression in salivary gland biopsies of Sjögren's syndrome. J Immunol 1994;152:5532–9.
19. Konttinen YT, Kemppinen P, Koski H, Li TF, Jumppanen M, Hietanen J, et al. T_H1 cytokines are produced in labial salivary glands in Sjögren's syndrome, but also in healthy individuals. Scand J Rheumatol 1999;28:106–12.
20. Price EJ, Venables PJ. The etiopathogenesis of Sjögren's syndrome. Semin Arthritis Rheum 1995;25:117–33.
21. Ozaki Y, Amakawa R, Ito T, Iwai H, Tajima K, Uehira K, et al. Alteration of peripheral blood dendritic cells in patients with primary Sjögren's syndrome. Arthritis Rheum 2001;44:419–31.
22. Ohyama Y, Nakamura S, Matsuzaki G, Shinohara M, Hiroki A, Fujimura T, et al. Cytokine messenger RNA expression in the labial salivary glands of patients with Sjögren's syndrome. Arthritis Rheum 1996;39:1376–84.
23. Miyake K, Moriyama M, Aizawa K, Nagano S, Inoue Y, Sadanaga A, et al. Peripheral CD4+ T cells showing a Th2 phenotype in a patient with Mikulicz's disease associated with lymphadenopathy and pleural effusion. Mod Rheumatol 2008;18:86–90.
24. Kanari H, Kagami S, Kashiwakuma D, Oya Y, Furuta S, Ikeda K, et al. Role of Th2 cells in IgG4-related lacrimal gland enlargement. Int Arch Allergy Immunol 2010;152 Suppl 1:47–53.
25. Zen Y, Fujii T, Harada K, Kawano M, Yamada K, Takahira M, et al. Th2 and regulatory immune reactions are increased in immunoglobin G4-related sclerosing pancreatitis and cholangitis. Hepatology 2007;45:1538–46.
26. Fujibayashi T, Sugai S, Miyasaka N, Hayashi Y, Tsubota K. Revised Japanese criteria for Sjögren's syndrome (1999): availability and validity. Mod Rheumatol 2004;14:425–34.
27. Vitali C, Bombardieri S, Jonsson R, Moutsopoulos HM, Alexander EL, Carsons SE, et al, and the European Study Group on the Classification Criteria for Sjögren's Syndrome. Classification criteria for Sjögren's syndrome: a revised version of the European criteria proposed by the American-European Consensus Group. Ann Rheum Dis 2002;61:554–8.
28. Greenspan JS, Daniels TE, Talal N, Sylvester RA. The histopathology of Sjögren's syndrome in labial salivary gland biopsies. Oral Surg Oral Med Oral Pathol 1974;37:217–29.
29. Daniels TE, Whitcher JP. Association of patterns of labial salivary gland inflammation with keratoconjunctivitis sicca: analysis of 618 patients with suspected Sjögren's syndrome. Arthritis Rheum 1994;37:869–77.

30. Szodoray P, Alex P, Jonsson MV, Knowlton N, Dozmorov I, Nakken B, et al. Distinct profiles of Sjögren's syndrome patients with ectopic salivary gland germinal centers revealed by serum cytokines and BAFF. Clin Immunol 2005;117:168–76.
31. Hiroki A, Nakamura S, Shinohara M, Gondo H, Ohyama Y, Hayashi S, et al. A comparison of glandular involvement between chronic graft-versus-host disease and Sjögren's syndrome. Int J Oral Maxillofac Surg 1996;25:298–307.
32. Sasaki M, Nakamura S, Ohyama Y, Shinohara M, Ezaki I, Hara H, et al. Accumulation of common T cell clonotypes in the salivary glands of patients with human T lymphotropic virus type I-associated and idiopathic Sjögren's syndrome. J Immunol 2000;164: 2823–31.
33. Kumamaru W, Nakamura S, Kadena T, Yamada A, Kawamura E, Sasaki M, et al. T-cell receptor Vβ gene usage by T cells reactive with the tumor-rejection antigen SART-1 in oral squamous cell carcinoma. Int J Cancer 2004;108:686–95.
34. Kawamura E, Nakamura S, Sasaki M, Ohyama Y, Kadena T, Kumamaru W, et al. Accumulation of oligoclonal T cells in the infiltrating lymphocytes in oral lichen planus. J Oral Pathol Med 2003;32:282–9.
35. Nakashima H, Miyake K, Moriyama M, Tanaka A, Watanabe M, Abe Y, et al. An amplification of IL-10 and TGF-β in patients with IgG4-related tubulointerstitial nephritis. Clin Nephrol 2010;73: 385–91.
36. Yamamura M, Modlin RL, Ohmen JD, Moy RL. Local expression of antiinflammatory cytokines in cancer. J Clin Invest 1993;91: 1005–10.
37. Morgan WS, Castleman B. A clinicopathologic study of Mikulicz's disease. Am J Pathol 1953;29:471–503.
38. Yamamoto M, Ohara M, Suzuki C, Naishiro Y, Yamamoto H, Takahashi H, et al. Elevated IgG4 concentrations in serum of patients with Mikulicz's disease. Scand J Rheumatol 2004;33: 432–3.
39. Yamamoto M, Harada S, Ohara M, Suzuki C, Naishiro Y, Yamamoto H, et al. Clinical and pathological differences between Mikulicz's disease and Sjögren's syndrome. Rheumatology (Oxford) 2005;44:227–34.
40. Kennedy MK, Torrance DS, Picha KS, Mohler KM. Analysis of cytokine mRNA expression in the central nervous system of mice with experimental autoimmune encephalomyelitis reveals that IL-10 mRNA expression correlates with recovery. J Immunol 1992;149:2496–505.
41. Rapoport MJ, Jaramillo A, Zipris D, Lazarus AH, Serreze DV, Leiter EH, et al. Interleukin 4 reverses T cell proliferative unresponsiveness and prevents the onset of diabetes in nonobese diabetic mice. J Exp Med 1993;178:87–99.
42. Firestein GS, Alvaro-Gracia JM, Maki R. Quantitative analysis of cytokine gene expression in rheumatoid arthritis. J Immunol 1990;144:3347–53.
43. Tsunawaki S, Nakamura S, Ohyama Y, Sasaki M, Ikebe-Hiroki A, Hiraki A, et al. Possible function of salivary gland epithelial cells as nonprofessional antigen-presenting cells in the development of Sjögren's syndrome. J Rheumatol 2002;29:1884–96.
44. Imai T, Baba M, Nishimura M, Kakizaki M, Takagi S, Yoshie O. The T cell-directed CC chemokine TARC is a highly specific biological ligand for CC chemokine receptor 4. J Biol Chem 1997;272:15036–42.
45. Imai T, Nagira M, Takagi S, Kakizaki M, Nishimura M, Wang J, et al. Selective recruitment of CCR4-bearing Th2 cells toward antigen-presenting cells by the CC chemokines thymus and activation-regulated chemokine and macrophage-derived chemokine. Int Immunol 1999;11:81–8.
46. Finkelman FD, Vercelli D. Advances in asthma, allergy mechanisms, and genetics in 2006. J Allergy Clin Immunol 2007;120: 544–50.
47. Meiler F, Klunker S, Zimmermann M, Akdis CA, Akdis M. Distinct regulation of IgE, IgG4 and IgA by T regulatory cells and Toll-like receptors. Allergy 2008;63:1455–63.
48. Shevach EM. $CD4^+$ $CD25^+$ suppressor T cells: more questions than answers. Nat Rev Immunol 2002;2:389–400.
49. Roncarolo MG, Levings MK. The role of different subsets of T regulatory cells in controlling autoimmunity. Curr Opin Immunol 2000;12:676–83.
50. Lan RY, Cheng C, Lian ZX, Tsuneyama K, Yang GX, Moritoki Y, et al. Liver-targeted and peripheral blood alterations of regulatory T cells in primary biliary cirrhosis. Hepatology 2006;43:729–37.
51. Miyoshi H, Uchida K, Taniguchi T, Yazumi S, Matsushita M, Takaoka M, et al. Circulating naive and $CD4^+CD^{25high}$ regulatory T cells in patients with autoimmune pancreatitis. Pancreas 2008; 36:133–40.